Ed è per la terza volta che mi riduco all'ultimo momento, come mio solito, nelle ultime correzioni della terza tesi della mia vita. Ma stavolta, al contrario delle due precedenti, voglio ringraziare tutti coloro che hanno permesso direttamente o indirettamente di farmi arrivare a questo traguardo (se qualcuno mi sfugge spero mi perdoni visto che sono le 3 del mattino):

Vorrei ringraziare di cuore:
- Mamma, per la rettitudine, l'amore, la forza, il coraggio;
- Papà, per avermi viziato;
- Riccardo, per le botte da orbi;
- Zia Anna, Simona e Cristina, per essere come mamma e sorelle;
- I nipotini per la gioia;
- Danièle, Roberto, Claire e Christine perché la famiglia non è solo genetica;
- Michela per l'affetto di una sorella;
- Danilo per la complicità di un fratello;
- Chiara, per il sostegno da vera sorella maggiore;

- Irene, per la sicura guida;
- LAB2, per molte cose;
- LAB2bis, per l'accoglienza;
- LAB9, per l'allegria;
- LAB6, per i reagenti;
- LABCell, per le ssscellule!!;
- Julie, per la pazienza;
- Chiara, Pinus, Lalla, Don Carlo, Peo, Adrino, Puzzola, Alberto, Aldo, Ale, Giulio, Marin per l'amicizia vera.
- Andrea, Manuela, Francesca, Ernesto, Simona per i primi passi;
- Emma, Marcella, Vera, Maria Rita per avermi indicato la via;
- Renato, Carlo, Francesca, Luca, Giorgia, Luca, Cristina, Shervin, etc… per la disciplina;

- Ines e Vittorio per aver badato a me come ad un figlio

Vorrei poi spendere le mie parole più preziose (anche perché oramai si sono fatte le 4) per dedicare questa tesi a colei che "mi ha scelto tra tanti", colei che sento sempre accanto, che saluto la mattina uscendo di casa e ritrovo al mio fianco al lavoro, il primo sguardo della mattina e l'ultimo della sera, la spalla forte su cui appoggiarmi in tutti i momenti in cui penso di non farcela; sapere che c'è qualcuno nel mondo che considera la mia vita più importante della sua. Ci siamo trovati ed abbiamo iniziato un percorso che spero poter percorrere insieme finché avrò vita.
A Marcella

Roma, 5 gennaio 2011

SAPIENZA
Università di Roma
Facoltà di Scienze Matematiche Fisiche e Naturali

DOTTORATO DI RICERCA
IN GENETICA E BIOLOGIA MOLECOLARE

XXIII Ciclo
(A.A. 2009/2010)

Role of microRNAs in Duchenne Muscular Dystrophy and in muscle differentiation

Dottorando
Davide Cacchiarelli

Docente guida
Prof. ssa Irene Bozzoni

Tutore
Prof. Antonio Musarò

Coordinatore
Prof. Irene Bozzoni

INDEX

ABSTRACT

Duchenne Muscular Dystrophy (DMD), caused by mutations in the dystrophin gene, is one of the most severe myopathies. Among different therapeutic strategies, exon skipping allows the rescue of dystrophin synthesis through the production of a shorter but functional mRNA. Making use of exon skipping strategy we demonstrated that in DMD, the absence of dystrophin at the sarcolemma delocalizes and downregulates Nitric Oxide Synthase (nNOS); this alters HDAC2 S-nitrosylation and its chromatin association. We show that the differential HDAC2 nitrosylation state in Duchenne versus wild-type conditions deregulates the expression of a specific subset of microRNA genes crucial in DMD physiopathology.
Namely, we identified miR-1 as regulator of the redox state of the cell through modulation of the G6PD enzyme while miR-29 controls the fibrotic process targeting extracellular matrix proteins.
We also show that, at variance with other myomiRs, miR-206 and miR-31 escape from the dystrophin-nNOS control being expressed in activated satellite cells before dystrophin expression. In these cells, miR-206 contributes to muscle regeneration through repression of the satellite specific factor Pax7, while miR-31 inhibits the early expression of dystrophin by directly repressing its mRNA.
Finally, in human DMD myoblasts treated with exon skipping molecules, we demonstrate that miR-31 inhibition increases dystrophin rescue representing a new approach to coadiuvate the existing therapeutic strategies.

We conclude that:

- the pathway activated by dystrophin/nNOS controls key miRNA circuitries increasing the robustness of the muscle differentiation programme.
- specific miRNAs are induced during muscle regeneration controlling the timing of mRNA expression during myoblasts differentiation.
- the inhibition of specific miRNA extression enhances dystrophin rescue obtained through exon skipping treatments.

INTRODUCTION

miRNA biogenesis and function

miRNAs are small, evolutionarily conserved noncoding RNAs, transcribed by RNA polymerase II. miRNAs display peculiar genic organization as they can be intergenic, exonic, intronic as monocistrnic or polycistronic units (Morlando et al., 2008; Ballarino et al., 2009).
Pri-miRNAs undergo a first endonucleolitic cleavage by the microprocessor complex (Drosha and DGCR8), which produces a 70 nucleotide hairpin RNA, termed pre-miRNA, which is subsequently exported to the cytoplasm and processed by Dicer to yield a duplex RNA 22-23 nucleotides long. Only one filament will be subsequently loaded into the silencing complex (RISC) as mature miRNA, while the other strand, the miRNA* will be degradated (Krol et al., 2010; Figure 1).
miRNAs regulate gene expression through sequence-specific interactions with the 3′ untranslated regions (UTRs) of target mRNAs resulting in translational repression or mRNA destabilization (Krol et al., 2010, Figure 1). The binding specificity to complementary target mRNAs is determined by Watson–Crick base-pairing of nucleotides 2–8 at the 5′ end of the miRNA, referred to as the ‘seed sequence’. miRNAs that share the same seed sequence are part of the same family and this means that they can act on the same target mRNAs.
While some miRNAs may exert their effects through pronounced repression of a relatively small number of mRNA targets, more commonly, miRNAs regulate dozens or hundreds of targets by relatively fine changes in expression. Thus, the summation of small changes in multiple mRNAs may be responsible for phenotypic effects of miRNAs. A recent study also demonstrated the ability of a miRNA to enhance translation, raising interesting new possibilities for the regulatory actions of miRNAs (Vasudevan et al., 2007) In addition, there is also evidence that small RNAs can directly control transcription through sequence-specific interactions with promoter elements of target genes (Schwartz et al., 2008). Perhaps, miRNAs can also function in a similar setting by directly conferring transcriptional, and post-transcriptional regulation on target genes.

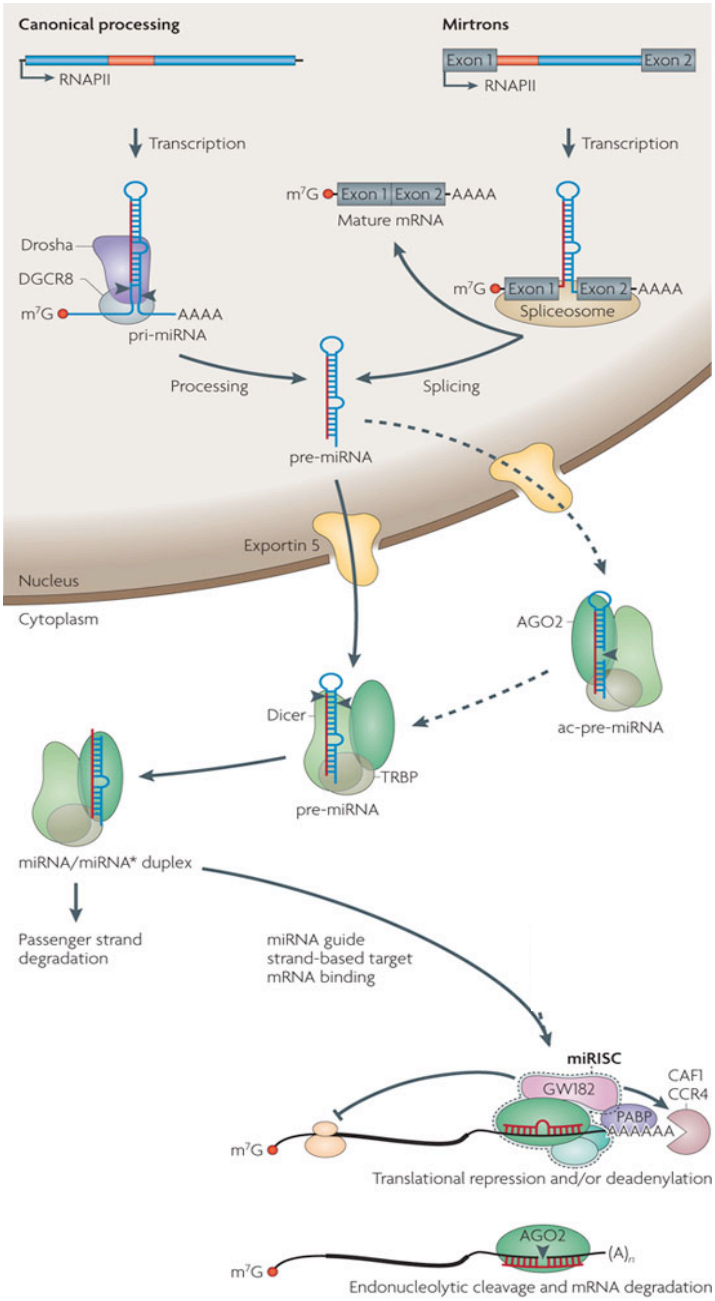

Figure 1: miRNA biogenesis (adapted from Krol et al., 2010)

Muscle-specific miRNA and their role in muscle development

Cardiac and skeletal muscle development are controlled by evolutionarily conserved networks of transcription factors that regulate the expression of genes crucial in coordinating processes like muscle growth, morphogenesis, differentiation, and contractility. For istance, in cardiac muscle MEF2 and the serum response factor (SRF) cooperatively activate cardiac gene expression by association with transcriptional co-activators. In skeletal muscle MEF2 activates the myogenic differentiation program in association with the basic-helix-loop-helix (bHLH) transcription factors, MyoD and myogenin (Potthoff & Olson, 2007). In addition to coordinate the expression of muscle genes, myogenic transcription factors also regulate the expression of a collection of microRNAs, which modulate at several levels muscle development and function.

An essential role for miRNAs in muscle development was shown by generating conditional null alleles of Dicer in cardiomyocytes and skeletal muscle, which results in severe muscle defects. These specific phenotipes are due to loss of miRNAs specifically expressed in cardiac and skeletal muscle (McCarthy JJ 2008).

Among these, the most widely studied are members of miR-1/206 and miR-133a/133b families, which originate from bicistronic transcripts (Figure 2) (Chen et al., 2006). miR-1-1 and miR-1-2 are identical and differ from miR-206 by four nucleotides, and miR-133a-1 and miR-133a-2 are identical and differ from miR-133b by two nucleotides. Cardiac and skeletal muscle specific transcription of miR-1-1/133a-2 and miR-1-2/133a-1 in vertebrates is controlled by two separate enhancers, one upstream and the other intergenic where the coordinated action of myogenic transcription factors SRF, MEF2, and MyoD has been reported (Figure 2) (Liu et al., 2007; Rao et al., 2006; Zhao et al., 2005).

The third cluster of muscle-specific miRNAs encoding miR-206 and miR-133b is expressed specifically in skeletal muscle (Chen et al., 2006) and its transcription is controlled by an upstream regulatory region enriched for MyoD association (Rao et al., 2006).

These miRNAs has been demonstrated to promote embryonic stem (ES) cells differentiation into mesodermal progenitors (Ivey et al., 2008) and myoblasts differentiation (Kim et al., 2006).

In vitro and in vivo studies have demonstrated that miR-1, miR-133a

and miR-206 regulate crucial aspects of muscle biology by targeting key regulators of muscle differentiation and proliferation (Figure 3 and reviewed in Williams et al., 2009)

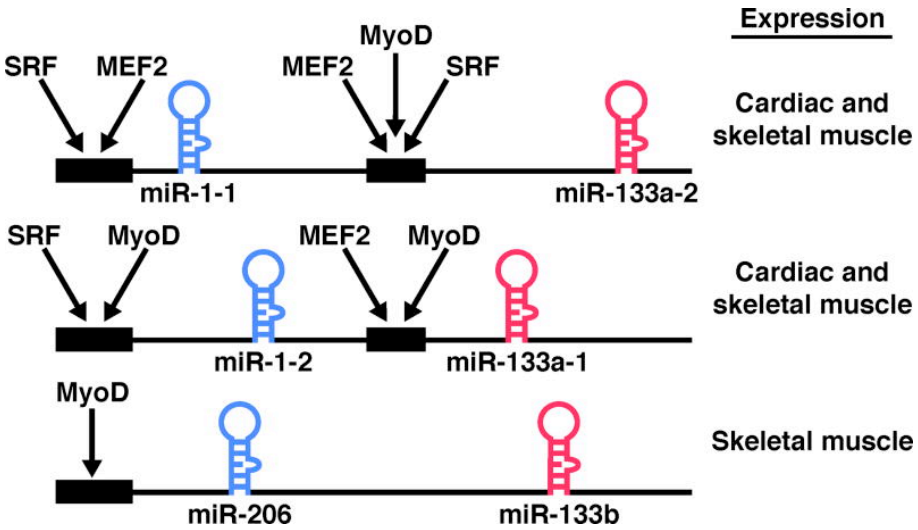

Figure 2. miRNA genomic organization (adapted from Williams et al., 2009)

Despite the fact that miR-1 and miR-206 belong to the same family an share the same mRNA targets in skeletal muscle, their specific action during muscle differentiation has still to be adressed.

Recently, it was discovered that myosin genes encode a new family of muscle specific miRNAs, the miR-208 family, which have important functions in regulating myosin content and stress-dependent cardiac remodeling (van Rooij et al., 2008).

In addition to muscle-specific miRNAs, there are also examples of ubiquitously expressed miRNAs that have been shown to have functions in muscle physiology like miR-214, miR-138 and miR-181 (reviewed in Williams et al., 2009).

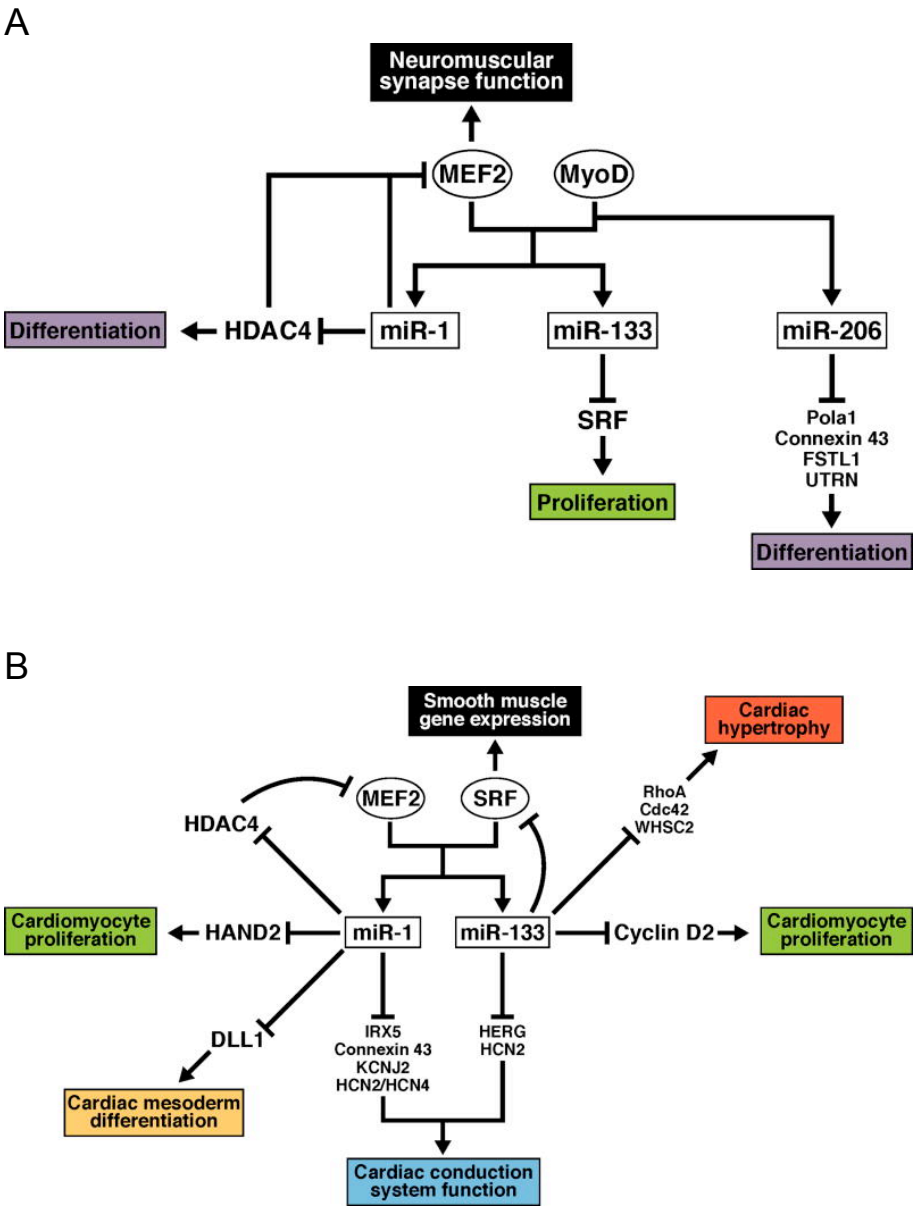

Figure 3. miRNA circuits during skeletal muscle (A) and cardiac (B) development (adapted from Williams et al., 2009)

miRNA in muscle disease

Several important studies have indicated that miRNA expression is dysregulated in cardiac and skeletal muscle disease and, in some cases, individual miRNAs have been shown to cause or alleviate disease. Global profiling of miRNAs in different forms of human heart disease demonstrated that miRNA gene expression signatures are diagnostic for distinct but related forms of heart disease (Ikeda et al., 2007). It has been elucidated the role of miR-195 to induce heart failure and the role of miR-29 downregulation, following myocardial infarction, to increase fibrosis (van Rooij et al., 2006 and 2008). Several studies were also focused on the identification of miRNAs dysregulated during skeletal muscle regeneration and muscular dystrophy. Kunkel and co-workers profiled miRNAs in muscle samples from a variety of human patients with primary muscle disorders and found a collection of miRNAs commonly dysregulated among patients affected by different types of muscle disorders (Eisenberg et al., 2007). For istance, the muscle-specific miR-206 was found to be upregulated in regeneratin fibers from dystrophin deficient mice (*mdx*) and WT mice treated with cardiotoxin, a potent inducer of muscle regeneration (Yuasa et al., 2008). The role of miR-206 in muscle regeneration and neuro-muscular junction formation has also addressed in mouse models for amyotrophic lateral sclerosis mouse model (Williams et al., 2009).
miRNA role was also studied in muscle neoplastic disease, like rhabdomyosarcoma which is caused by proliferation of muscle progenitor cells, where miR-29 and miR-206 act as tumor suppressor genes (Wang et al., 2008; Taulli et al., 2009).
Several strategies have been developed to manipulate miRNA expression. A pharmacological approach is represented by the use of oligonucleotides which mimic miRNA sequence to overdose a specific miRNA or a complementary miRNA sequence to sequester it (Krutzfeldt et al., 2005). Also gene theraphy strategies have been developed to modulate miRNA expression using specific constructs to overexpress pri-miRNA sequences (Fati et al., 2005) or decoy mRNAs with artificial miRNA target sites to sequester endogenous miRNAs (Gentner et al., 2009).

Duchenne Muscular Dystrophy and gene therapy approaches

Duchenne Muscular Dystrophy (DMD) is an X-linked recessive disorder caused by mutations in the dystrophin gene (DMD) that affects 1/3500 males. This life-threatening disease is characterized by rapid and progressive skeletal muscle degeneration, leading to loss of ambulation and death. Dystrophin gene encodes for a 427 kDa protein that links the cytoskeleton to a complex of proteins (Dystrophin-Associated Protein Complex - DAPC) on the membrane of muscle fibers (Matsumura et al., 1994; Figure 4). The principal role of DAPC is to connect intracellular actin microfilaments to the extracellular matrix determining a structural stabilization of the sarcolemma (Ervasti et al., 2008). The absence of Dystrophin in DMD patients leads to delocalization of the entire DAPC. As a consequence, muscle fibers become more sensitive to mechanical damage leading to muscle degeneration, chronic inflammation, susceptibility to oxidative stress and increased fibrosis, all of which exacerbate the dystrophic phenotype.

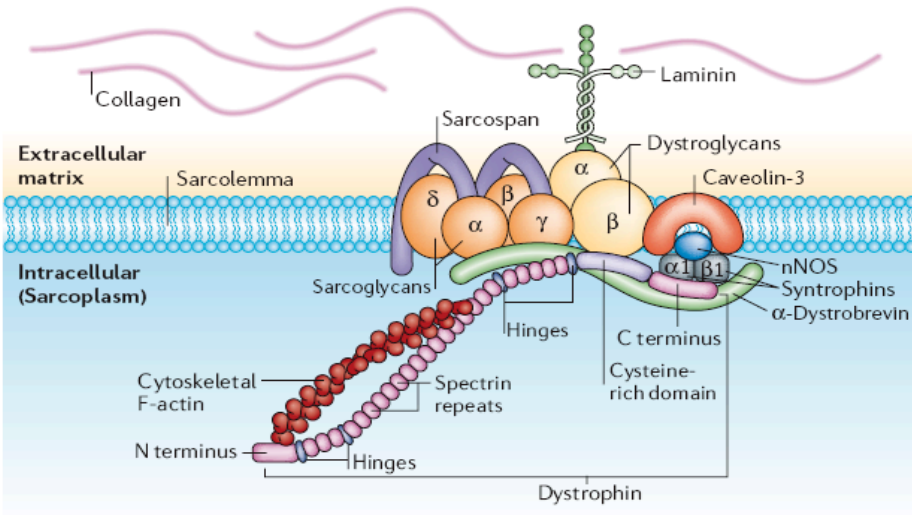

Figure 4. The Dystrophin-Associated Protein Complex (DAPC)

The majority of DMD patients carry mutations that disrupt the reading frame of the dystrophin gene, resulting in truncated dystrophin that lacks the C-terminal bridging domain (Figure 5A) (Aartsma-Rus et al., 2006). Interestingly, Becker muscular dystrophy (BMD) (Koenig et al., 1989), a milder allelic disease, is frequently due to mutations that maintain the DMD reading frame but result in an internally truncated dystrophin protein that only lacks part of the central rod domain. These observations have led to the concept that it is possible to use, either for gene replacement or in exon-skipping strategies, a dystrophin protein with a partially deleted flexible central rod domain. Indeed, several functional studies have determined that relatively large internal segments of the DMD gene can be deleted without dramatically reducing functionality (Athanasopoulos et al., 2004).

Over the past 20 years, the *mdx* mouse, carring a stop codon inside exon 23 of the dystrophin gene, has been widely used as animal model of DMD pathology. Moreover, it provides a convenient system to test possible therapeutic interventions and select molecular markers to monitor disease progression and therapeutic outcomes.

Modifying the primary mRNA sequence is the first opportunity to intervene and correct mutations at the RNA level. It has been shown that most of the mutations in the dystrophin gene can be "cured" at the post-transcriptional level by preventing the inclusion of specific mutant exons in the mature mRNA and recovering a functional open reading frame (Aartsma-Rus et al., 2009). The exon-skipping strategy allows the production of a shorter but still functional dystrophin as a BMD-like phenotype. In theory, single and double exon skipping would be applicable to 83% of all DMD mutations (Aartsma-Rus et al., 2009) . The exon skypping approach was initially achieved by the use of antisense oligonucleotides complementary to the splice junctions of the exon to exclude. This successful *in vitro* strategy addresses *in vivo* hurdles such as whole body delivery and long-term expression. These issues have been improved by using expression cassettes to drive the expression of the antisense molecules under the U1 small nuclear RNA regulatory elements (Figure 5B). This approach was able to rescue dystrophin in cultured myoblasts from DMD patients (De Angelis et al., 2002) and in *mdx* mouse via adeno-associated virus (AAV) delivery allowing the recovery of dystrophin in a body wide manner (Denti et al., 2006 and 2008).

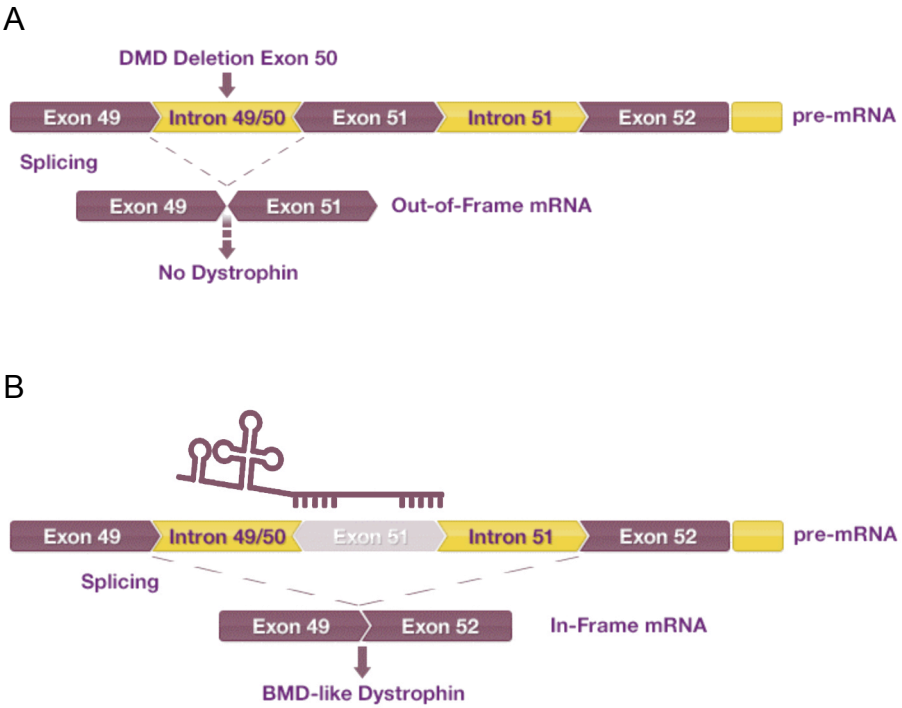

Figure 5. Example of exon-skipping strategy.
(A) Deletion of exon 50 in DMD gene results in an out-of-frame mRNA transcript and a prematurely aborted dystrophin synthesis. (B) Employing of antisense molecules against exon 51 splice sites produce an in frame mRNA transcript resulting in a shortened BMD-like dystrophin protein.

Histone Deacetylases and Nitric Oxide in Duchenne pathology

Histone deacetylases (HDACs) are a family of enzymes divided in four sub-classes defined according to structural similarities. They are principally involved in the withdrawal of acetyl-groups from a large number of proteins including nuclear core histones. Their pivotal role in regulating the acetilation state of chromatin resulted in a direct control of chromatin accessibility and dinamics. The presence of such a cohort of molecules with apparent similar enzymatic activity may be incorrectly interpreted as redundancy while it probably reflects very specialized functions.
Due to their crucial role in epigenetic regulation of gene expression, HDACs have been selected as one of the first molecular targets to develop new epigenetically active drugs. In fact, HDAC inhibitors are now widely used in several cancer therapies as a consequence of their anti-proliferative and pro-apoptotic properties (Jung et al., 2001). Moreover, recent observations enlightened the important therapeutic effects of HDAC inhibitors in experimental animal models for arthritis, neurodegenerative and neuromuscular disorders, heart ischemia, cardiac hypertrophy, heart failure and arrhythmias (reviewed in Colussi et al., 2010).
Recently, HDAC inhibitors have been found particularly effective in the mdx mouse model of DMD disease where they promote rescue of dystrophic phenotype (Minetti et al., 2006). In line with this, the same effect was also observed by administration of nitric oxide (NO) donors (Colussi et al., 2008 and 2009).
NO has emerged as a key second messenger molecule in serveral cellular pathways. Its production in muscle is granted by the activity of a neuronal/muscular specific isoform, nNOS, which directly interacts with dystrophin in the DAPC. In DMD muscles the dystrophin absence at sarcolemma causes the mislocalization of the entire DAPC including nNOS and the consequent impairing in NO production (Brenman et al., 1995).
Finally, a link between HDAC inhibitors and NO has been reported by the identification of the common cellular target, the HDAC2 enzyme.
While HDAC inhibitors act inactivating all members of HDAC family by blocking the catalityc active site, NO inhibits specifically HDAC2. In fact, HDAC2 S-nitrosilation on two Cys residues

(Cys262 and Cys274) determines conformational changes in the enzyme which induce its release from chromatin and a consequent increase in chromatin accessibility (Nott. et al., 2008)
In Duchenne pathology in fact, the reduction of NO production due to DAPC delocalization, resulted in HDAC2 S-nitrosylation-dependent inhibition with a consequent aberrant deacetylase activity (Colussi et al., 2008).
By promoting muscle regeneration, follistatin was identified as HDAC2 target and it represents a mediator of therapeutic effects observed upon NO and HDAC inhibitors treatments (Minetti et al., 2006). However, follistatin rescue *per se* is not suffcient to justify the global amelioration in terms of fibrosis and oxidative stress observed in *mdx* treated fibers. At the moment molecular mechanisms underlining physiopathology of HDAC2 action in DMD have to be still investigated.

AIMS

This work started with the observation that upon dystrophin recovery in exon skipped treated *mdx*, low levels of dystrophin expression (5–10%), are sufficient to confer a long-term benefit to the entire muscle from morphological and functional perspectives (Denti et al., 2006 and 2008). So out principal aim was to study if dystrophin, beside its well defined structural role, could co-operate in signal transduction processes justifying as low protein recovery, observed upon exon skipping treatments, could rescue DMD phenotype almost to healty levels. We choose to study the role of miRNA, as putative targets of this suggested pathway, both in muscle fibers and muscle stem cells.

RESULTS

The expression levels of specific miRNAs correlate with the amount of dystrophin

Six-week old *mdx* animals were tail vein injected with a recombinant adeno-associated viral vector carrying a U1-chimeric antisense construct (AAV#23, Figure 6A) previously reported to induce the skipping of the mutated exon 23 and to restore dystrophin synthesis (Denti et al., 2006). After 1 month, *mdx* and AAV#23-treated *mdx* siblings were sacrificed in parallel with wild type (WT) isogenic/aged matched animals. Different muscular districts (gastrocnemius, diaphragm, triceps and quadriceps) were dissected and tissue collected for protein, RNA and chromatin analyses. Western blot revealed that through the exon skipping treatment, rescue of dystrophin was obtained in all districts (Figures 6B shows data relative to gastrocnemius), confirming the previously described body-wide activity of the AAV#23 virus. Due to individual variability in the systemic delivery of AAV, we were able to classify injected animals in three different groups (G1, G2 and G3), which displayed ≤1%, 1-5% and 5-10% of dystrophin rescue, respectively. A representative sample of each group is shown in Figure 6B.
Real-time based low density arrays revealed that the expression of a subset of miRNAs deregulated in *mdx* animals, was restored towards WT levels in AAV#23-treated mice (data not shown).
Among the miRNAs analyzed by array, we validated by qRT-PCR those showing the most prominent variations. Since homologous members of miR-29, miR-30 and miR-133 families were equally deregulated, we focused our analysis on one member per family. The muscle-specific (myomiR) miR-1 and miR-133 and the ubiquitous miR-29c and miR-30c, down-regulated in *mdx,* recovered towards WT levels in exon skipping-treated animals (shown in blue in Figure 6C),. A direct correlation between miRNA levels and dystrophin rescue was observed: G1 animals showed a very limited miRNA recovery, while G3 displayed levels close to WT ones .
At variance with the other myomiRs, miR-206 and miR-31 were highly expressed in *mdx* as well as in AAV#23-treated animals. (shown in green in figure 6C)

The inflammatory miR-223 (Fazi et al., 2005), specific of granulocytic lineage, was found to be very abundant in *mdx* muscles and proportionally reduced in the three groups of treated animals (shown in red in Figure 6C); its decrease in AAV#23-*mdx* is consistent with the observed amelioration of the inflammatory state of the muscle due to dystrophin rescue (Denti et al., 2008; Aartsma-Rus et al., 2009). Finally, the expression levels of the ubiquitous miR-23a and miR-27a were unchanged in WT and *mdx*, as well as in treated animals.

The relative changes in the expression patterns of miR-1, miR-29, miR-206, and miR-223 observed in the gastrocnemius were confirmed in other muscle districts (data not shown), demonstrating that the miRNA expression profile correlated with dystrophin rescue in a body-wide manner.

The observation that the expression of a specific subset of miRNAs varies in response to the presence of dystrophin, prompted the analysis in a human Duchenne model system. Differentiating DMD myoblasts, carrying a deletion of exons 48-50, were treated with a lentiviral construct expressing an antisense RNA able to induce exon 51 skipping (LV#51) or with an empty vector (LV-mock). This treatment was previously shown to produce an in frame mRNA and to rescue dystrophin synthesis (De Angelis et al., 2002; Incitti et al., 2010). According to the *mdx* model, when dystrophin synthesis was restored (Figure 6D), the levels of miR1, miR-133a, miR-29c, miR-30c and miR-206 increased, while miR-23a expression did not change (Figure 6E).

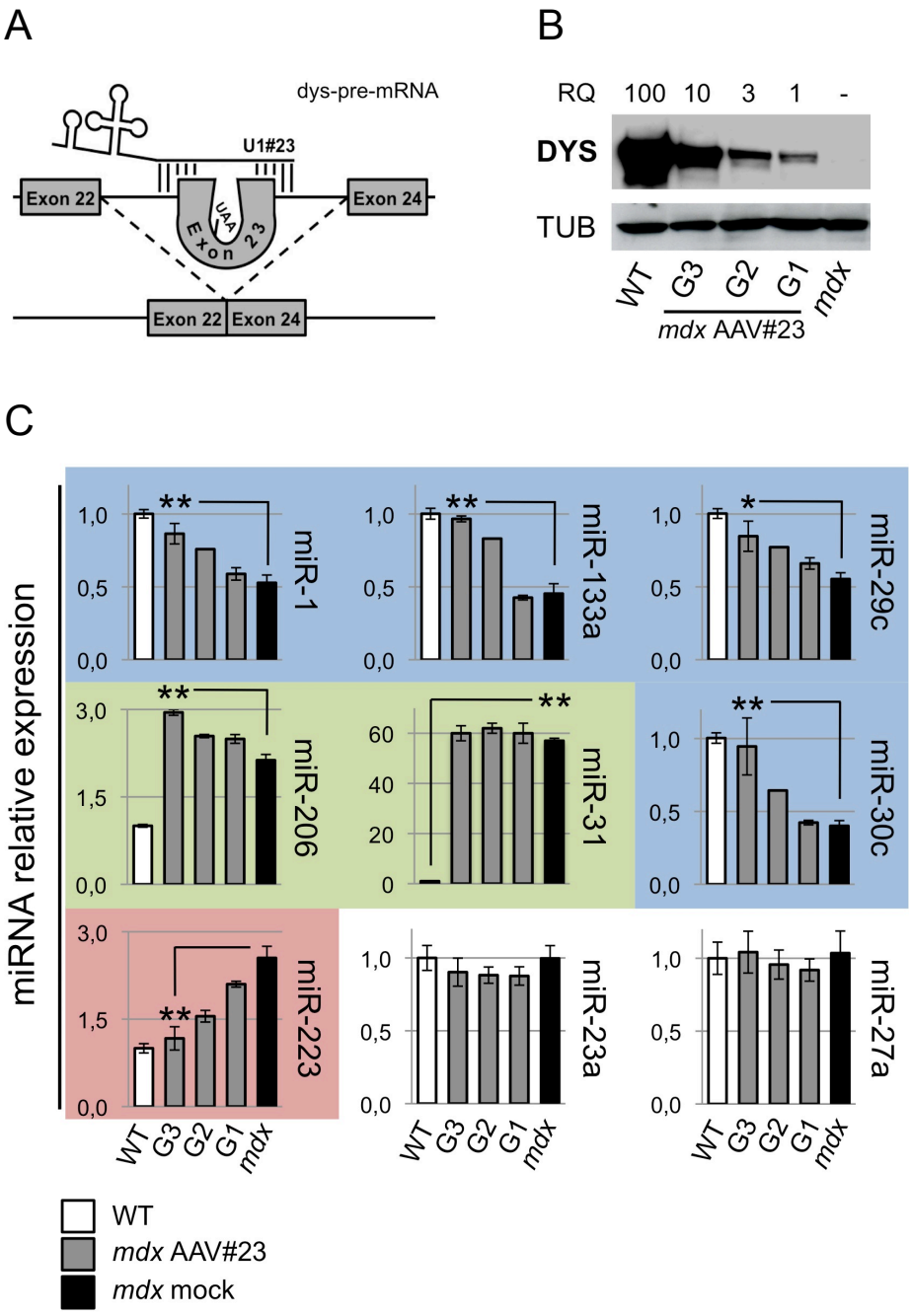
A
dys-pre-mRNA
U1#23
Exon 22
Exon 24
UAA
Exon 23
Exon 22 Exon 24
B
RQ 100 10 3 1 -
DYS
TUB
WT G3 G2 G1 mdx
mdx AAV#23
C
miRNA relative expression
miR-1
miR-133a
miR-29c
miR-206
miR-31
miR-30c
miR-223
miR-23a
miR-27a
WT G3 G2 G1 mdx
WT
mdx AAV#23
mdx mock

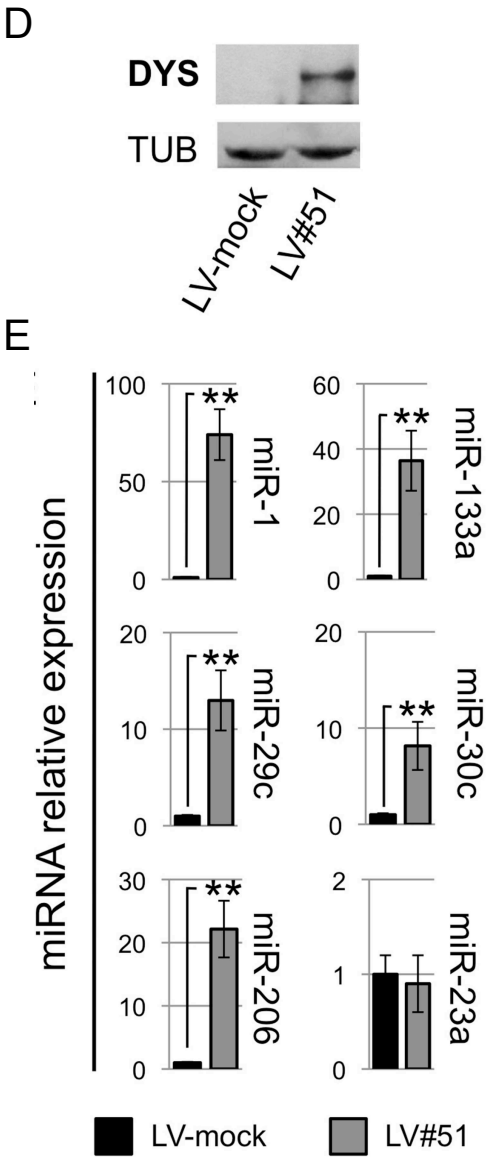

Figure 6. microRNA expression in Duchenne Muscular Dystrophy.
(A) Schematic representation of the exon skipping strategy for *mdx* mutation. (B) Western blot with anti-dystrophin (DYS) and anti-tubulin (TUB) antibodies performed on protein extracts from the gastrocnemius of WT, *mdx* and AAV#23-treated *mdx* (G1, G2 and G3) animals, sacrificed 4 weeks after systemic virus injection. Dystrophin relative quantifications are shown on the top of each lane. (C) Histograms show miRNA relative expression in WT, G1-G3 and *mdx* mice, measured by qRT-PCR. miR-23a and miR-27a were used as controls. Expression levels were normalized to snoRNA55 and shown with respect to WT set to a value of 1. (D) Western blot with DYS and TUB antibodies on protein extracts from human DMD myoblasts infected with LV#51 (LV#51) or control (LV-mock) lentiviruses and differentiated for 7 days. (E) Histograms show miRNA relative expression in LV-mock and LV#51 treated DMD cells measured by qRT-PCR. U6 snRNA was used as endogenous control. Relative expressions are shown with respect to LV-mock DMD cells, set to a value of 1. One asterisk ($p<0.05$), two asterisks ($p<0.01$).

HDAC2 controls the expression of specific miRNA genes

Immunofluorescence analyses (Figure 7A) were performed with anti-dystrophin and anti-nNOS antibodies on sections from the gastrocnemius of WT, *mdx* and G3 *mdx* (AAV#23). Upon exon skipping treatment, dystrophin synthesis and its correct localization to the periphery of the fibers was obtained (DYS); moreover, the restoration of dystrophin paralleled the proper co-localization of nNOS to the DAPC (nNOS). The morphological amelioration of the muscles transduced with AAV#23 was also observed by haematoxylin and eosin staining (data not shown).
One interesting target of nNOS was found to be the HDAC2 chromatin remodelling enzyme (Nott et al., 2008; Colussi et al., 2008). Therefore, we tested whether HDAC2 was differentially nitrosylated in WT, *mdx*, and AAV#23-treated *mdx* animals. Protein muscle extracts were immunoprecipitated with anti-nitroso-cysteine antibody and subsequently analyzed by Western blot for HDAC2. The lowest level of nitrosylated HDAC2 was found in *mdx* mice; progressive increase of HDAC2 nitrosylation was detected in AAV#23 and WT muscles (Figure 7B). These data provided a correlation between nitrosylation state of HDAC2 and dystrophin levels. Since the nitrosylation state of HDAC2 was found to affect its association to the chromatin (Nott et al., 2008), we tested whether altered levels of miRNAs in *mdx* were due to HDAC2 recruitment to their promoters. We selected the miR-1 and miR-29 promoters since they have been previously characterized (Rao et al., 2006; Liu et al., 2007; Wang et al., 2008). ChIP analysis with antibodies against RNA polymerase II and AcH3K9 showed low binding levels in *mdx* and progressive increase in G3 (AAV#23) and WT animals (Figure 7C). These data indicated a good correlation between the transcriptional state of these loci and the expression levels of the corresponding miRNAs (Figure 6C), confirming that variations in miRNA expression depended on transcriptional control. ChIP with anti-HDAC2 antibody revealed its specific binding with miR-1 and miR-29 promoters only in *mdx* mice (Figure 7C) where these miRNAs are down-regulated. No reactivity was observed with either HDAC1 or HDAC4 (data not shown). On the contrary, the miR-206 promoter (characterized by MC and DC - personal communication) did not reveal any HDAC2 interaction.

ChIP analysis were carried out also in human differentiating DMD myoblasts infected with the lentiviral construct expressing an antisense RNA (LV#51) able to rescue dytrophin synthesis. The results indicated that also in this system the up-regulation of miR-1 and miR-29 correlated with release of HDAC2 from their promoters and changes in histone acetylation state (Figure 7D). Also in DMD cells no HDAC2 interaction was detected on miR-206 promoter. These data indicate that both in murine and human dystrophic cells the absence of dystrophin correlates with HDAC2 binding to a specific subset of miRNAs, while, upon dystrophin rescue, HDAC2 is released from these promoters.

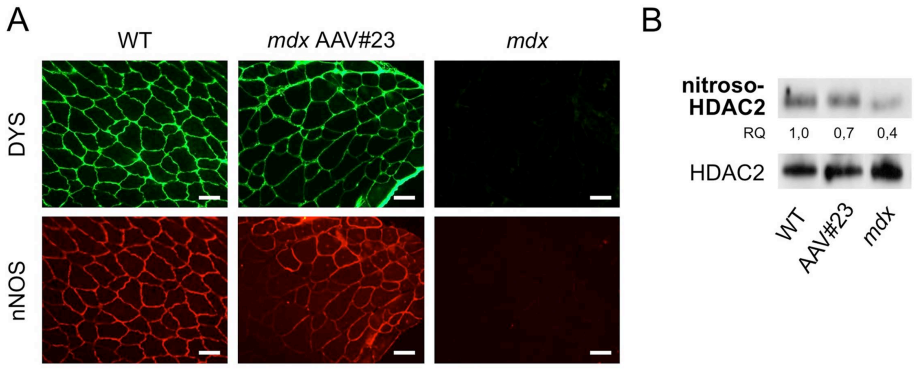

Figure 7. Dystrophin/nNOS re-localization modulates HDAC2 occupancy on miRNA loci.
(A) Gastrocnemius from WT, AAV#23-treated *mdx* and control *mdx* mice were analyzed by immunofluorescence with DYS and nNOS antibodies. Original magnification, X20. Scale bar 100 μm. (B) Protein extracts from the gastrocnemius of WT, AAV#23-treated *mdx* (AAV#23) and control *mdx*, were immunoprecipitated with antibody against nitrosylated-Cys residues and assayed for HDAC2 by Western blot (nitroso-HDAC2). Below each lane the relative quantities (RQ) with respect to WT are indicated. Values are normalized for the amount of total HDAC2 (HDAC2) and represent the average of three independent experiments.

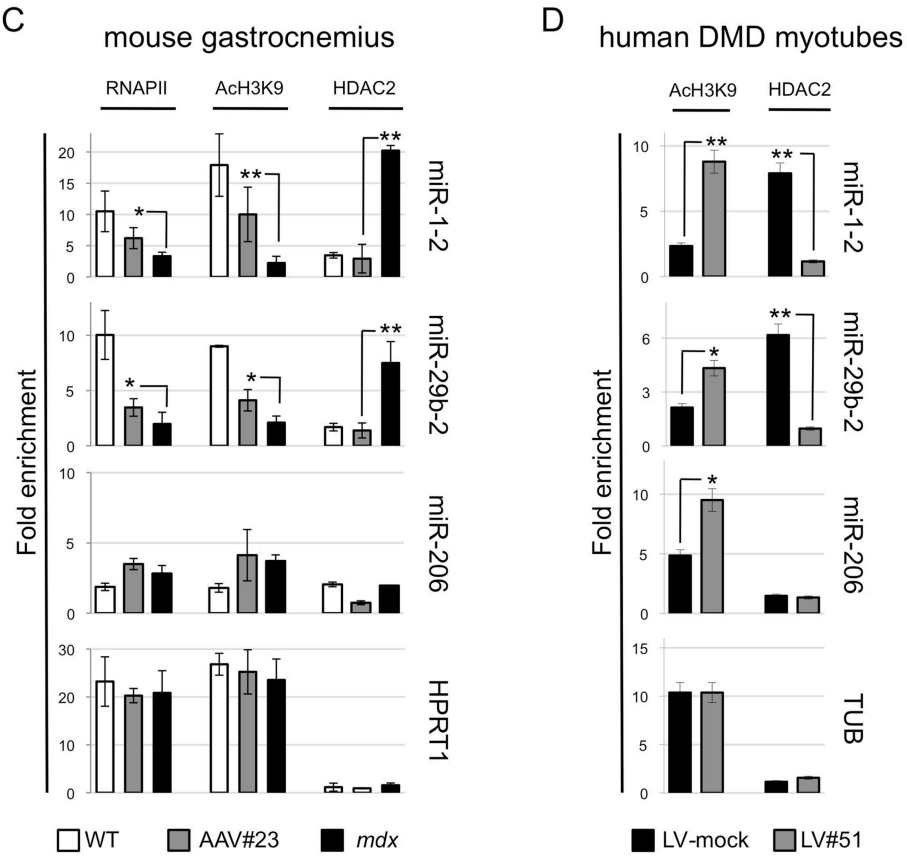

(C-D) ChIP analyses performed on miR-1-2/133a, miR-29b-2/29c and miR-206 promoters. (C) Histograms show RNA polymerase II (RNAPII), AcH3K9 and HDAC2 enrichments in WT, AAV#23 and *mdx* gastrocnemius. (D) Histograms show AcH3K9 and HDAC2 enrichments in control (LV-mock) and antisense-treated (LV#51) DMD myoblasts. HPRT1 and tubulin (TUB) promoter regions were used as unrelated transcriptional units, while 5,8S rRNA and tRNA genes were used as internal negative controls. Results are expressed as fold-enrichment of DNA immunoprecipitated samples relative to INPUT chromatin. One asterisk ($p<0.05$), two asterisks ($p<0.01$).

Nitric Oxide (NO) signalling controls miRNA expression through HDAC2 modification

Local injection of the NO-donor nitroglycerin (NTG) was utilized as a way of inducing NO-response to specific body districts. Leg muscles of *mdx* animals were injected with NTG, or physiological solution as control, and dissected after 4 hours. Immunoprecipitation with antibody against nitrosylated cysteine residues and subsequent HDAC2 Western blot analysis, indicated that NTG treatment rescues the nitrosylated levels of HDAC2 to wild type values (Figure 8A). qRT-PCR and ChIP analysis were performed to measure miRNA levels and HDAC2 association to the corresponding promoters. The data show that NTG treatment in *mdx* mice: i) increases miR-1 and miR-29 expression (Figure 8B); ii) induces HDAC2 release from the promoters of these miRNAs (Figure 8C); iii) has no effect on miR-206.
To further prove the role of HDAC2 nitrosylation on miRNA control, *mdx* muscles were electroporated with expression cassettes encoding for a wild type flagged-HDAC2 protein or for a derivative mutated at the two cysteines (Cys 262 and Cys 274) known to be the target of nitrosylation (Nott et al., 2008). Two weeks after treatment, NTG was locally injected and samples extracted for protein, RNA and chromatin analyses. Figure 8D shows that both exogenous proteins are expressed in the electroporated tissues (Flag-HDAC2) and only the wild type form can be nitrosylated (nitroso Flag-HDAC2). ChIP experiments with anti-flag antibodies showed that, upon NTG treatment, wild type Flag-HDAC2 was released from miR-1 and miR-29 promoters (Figure 8F) paralleling the increase of the corresponding miRNAs (Figure 8E); on the contrary, the mutant Flag-HDAC2 protein was still associated to the promoters producing their down-regulation (Figure 8E and 8F). No differences were observed on the HDAC2-independent miR-206 promoter.
Altogether, these results demonstrate that Nitric Oxide induces HDAC2 nitrosylation, thus regulating its binding on specific miRNA promoters.

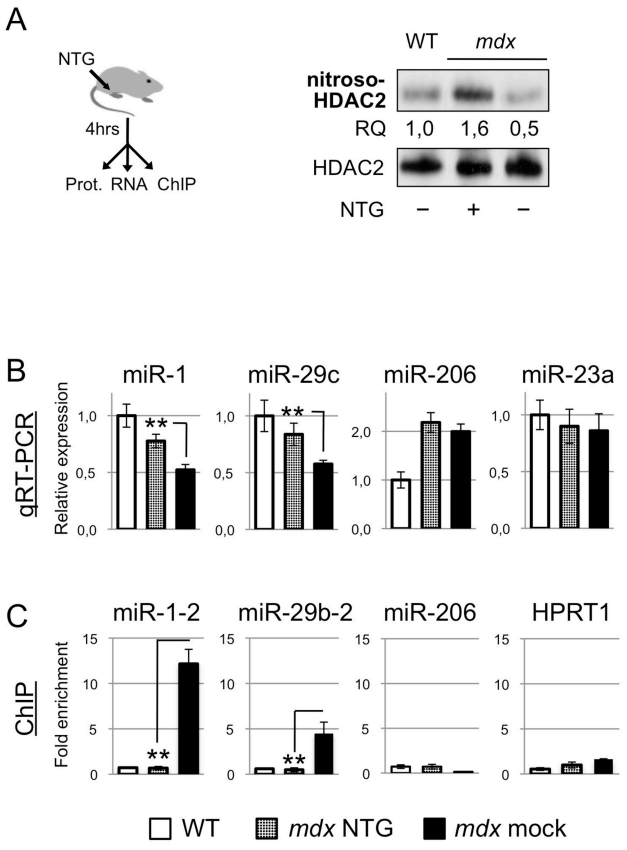

Figure 8. NO signalling controls miRNA expression trough HDAC2 nitrosylation.

(A-C) mice were injected with nitroglycerin (NTG) into the right gastrocnemius and with physiological solution into the left one. After 4 hours, protein, RNA and chromatin samples were collected. (A, right panel) Proteins were immunoprecipitated with antibody against nitrosylated-Cys residues and assayed for HDAC2 by Western blot (nitroso-HDAC2). Below each lane the relative quantities (RQ) with respect to WT are indicated; values are normalized for the amount of total HDAC2 (HDAC2) and represent the average of three independent experiments. (B) Histograms show miRNA relative expression measured by qRT-PCR in NTG-treated (*mdx* NTG) or mock injected (*mdx* mock) *mdx* muscles with respect to WT one set to a value of 1. Relative expressions were normalized to snoRNA55. (C) ChIP analyses for HDAC2 on miR-1-2/133a, miR-29b-2/29c and miR-206 promoters in WT, *mdx* NTG and *mdx* mock muscles. HPRT1 promoter region was used as unrelated transcriptional unit while 5,8S rDNA was used as an internal negative control. Results are expressed as fold-enrichment of DNA immunoprecipitated samples relative to INPUT chromatin.

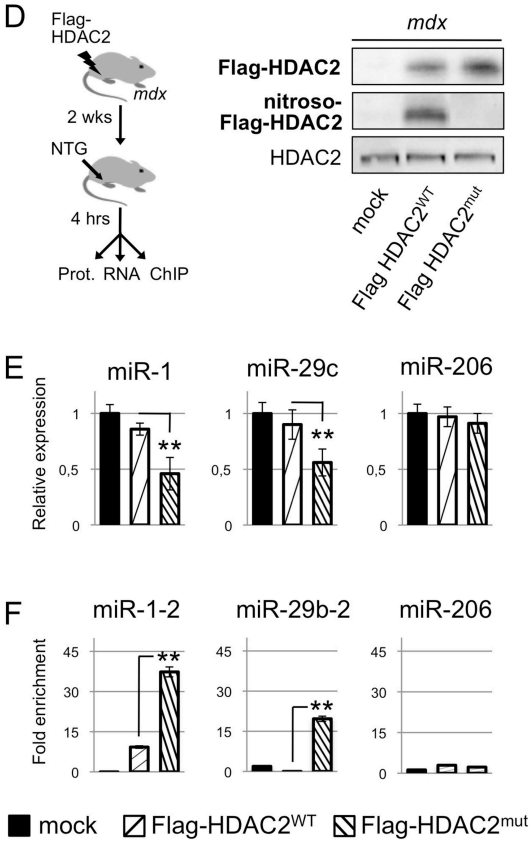

(D-F) *mdx* mice were electroporated into the right tibialis with expression cassettes encoding for a wild type flagged HDAC2 protein (Flag-HDAC2^{WT}) or for a derivative mutated at Cys262 and Cys274 (Flag-HDAC2^{mut}). After 2 weeks mice were injected with NTG into the right tibialis and with physiological solution into the left one (mock). After 4 hours protein, RNA and chromatin samples were collected. (D, right panel) Expression levels of flagged HDAC2 were assayed by Western Blot with anti-Flag antibody (Flag-HDAC2). Nitrosylation state was revealed by immunoprecipitation with anti-FLAG antibody followed by Western blot using an antibody against nitrosylated-Cys residues (nitroso-Flag-HDAC2). (E) Histograms show miRNA relative expression measured by qRT-PCR in mock, Flag-HDAC2^{WT} and Flag-HDAC2^{mut} treated muscles. Expression levels were normalized to snoRNA55 and shown with respect to mock set to a value of 1. (F) ChIP analyses were performed with anti-Flag antibody on miR-1-2/133a, miR-29b-2/29c and miR-206 promoters in mock, Flag-HDAC2^{WT} and Flag-HDAC2^{mut} treated muscles. Results are expressed as fold-enrichment of DNA immunoprecipitated samples relative to INPUT chromatin. Two asterisks ($p<0.01$).

miR-1 controls G6PD, a relevant enzyme in the response to oxidative stress

In silico analysis, performed by comparing mRNA expression profiles in wild type versus *mdx* animals (Tseng et al., 2002), identified a large number of predicted targets of those miRNAs showing the highest variations in our analysis. For the down-regulated miR-1, miR-29 and miR-30, several up-regulated targets relevant in muscle physiology were found, such as those involved in energetic metabolism, cytoskeleton remodelling, extracellular matrix and transcriptional regulation in muscle (Figure 10).
One important issue in dystrophic muscles is their susceptibility and response to oxidative stress suggested to be involved in disease progression (Rando et al., 1998). Glucose-6-Phosphate Dehydrogenase (G6PD) mRNA, deregulated in *mdx* muscles, contains in its 3'UTR three putative binding sites for the miR-1 family (see Figure 9A). G6PD is a cytosolic enzyme in the pentose phosphate pathway that supplies reducing energy to cells by maintaining the level of NADPH which in turn ensures high ratio between reduced and oxidized glutathione (GSH/GSSG). GSH represents the major antioxidant molecule that protects cells against oxidative damage.
Luciferase reporter assays validated G6PD mRNA as target of the miR-1 family. Figure S9 shows that miR-1 and miR-206, are able to repress luciferase activity only in the presence of a wt G6PD-3'UTR and that this repression is alleviated by anti-miR-1 and anti-miR-206 LNA oligonucleotides.
Several data indicated an inverse correlation between G6PD and miR-1 expression: *in vitro* differentiation of C2 myoblasts showed that the increase in miR-1 levels (Figure 11A, upper panel) correlated with decrease of G6PD protein (Figure 11A, middle panel), and GSH/GSSG ratio (Figure 11A, lower panel). Figure 11B shows that in *mdx* mice, where miR-1 is down-regulated, G6PD was detected at higher levels than in WT muscles; whereas, in AAV#23-treated *mdx*, in which miR-1 resumes, the amount of G6PD was reduced. Notably, in *mdx* mice, increase in G6PD levels was accompanied by a decrease in GSH/GSSG ratio (Figure 11B, lower panel). This apparent contradiction can instead be explained considering that in *mdx* muscles, most of the NADPH is utilized in the O_2 to $O^{\circ-}_2$ conversion

mediated by the Ca^{++}-dependent activation of NADPH oxidase (NOX; Shkryl et al., 2009). Detoxification of the superoxide radical could further reduce NO levels already low in *mdx*. Therefore, we asked whether interfering with this pathway could affect the nitrosylation state of HDAC2. When G6PD was inactivated through administration of 6-aminonicotinamide (6-AN; Walker et al., 1999), HDAC2 nitrosylation increased as well as the levels of miR-1 (Figure 11C). In line with this, NOX inhibition with apocynin (APO; Gupte et al., 2006) also increased HDAC2 nitrosylation and miR-1 levels (Figure 11C). Finally, G6PD down-regulation through over-expression of miR-1 (p-miR-1) in *mdx* muscles increased HDAC2 nitrosylation with respect to control (Figure 11D). The link between G6PD, NO, HDAC2 and miR-1 in *mdx* is shown in Figure 11E; namely, in conditions of increased levels of G6PD more $O^{\circ-}_2$ radicals, deriving from the activity of NOX, are converted to $ONOO^{\circ-}$. This reduced both NO levels and HDAC2 nitrosylation.
Altogether, these data demonstrate that all these components are on the same pathway and that a feed forward control between G6PD and miR-1 through the S-nitrosylation of HDAC2 exists.

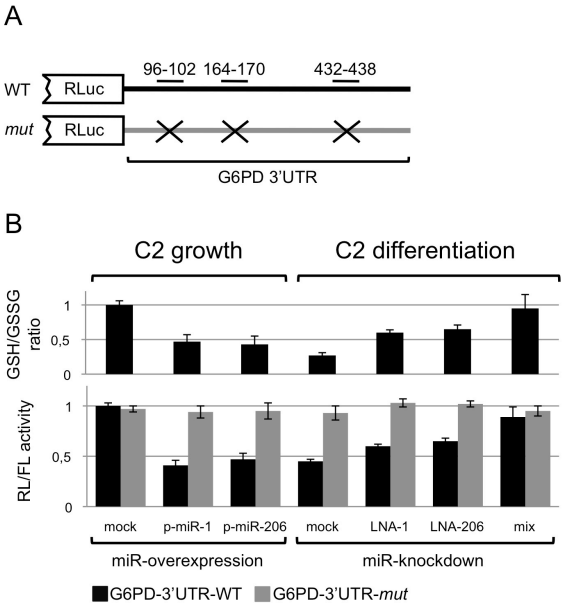

Figure 9. G6PD is target of miR-1 family. (A) Luciferase reporter with wild type G6PD 3'UTR or mutated for miR-1 target sites (B) Luciferase activity and GSH/GSSG ratios tested in C2 myoblasts in growth medium, in presence of miR-1 and miR-206 over-expression, and in differentiation medium, in presence of LNA oligos against miR-1, miR-206 or both.

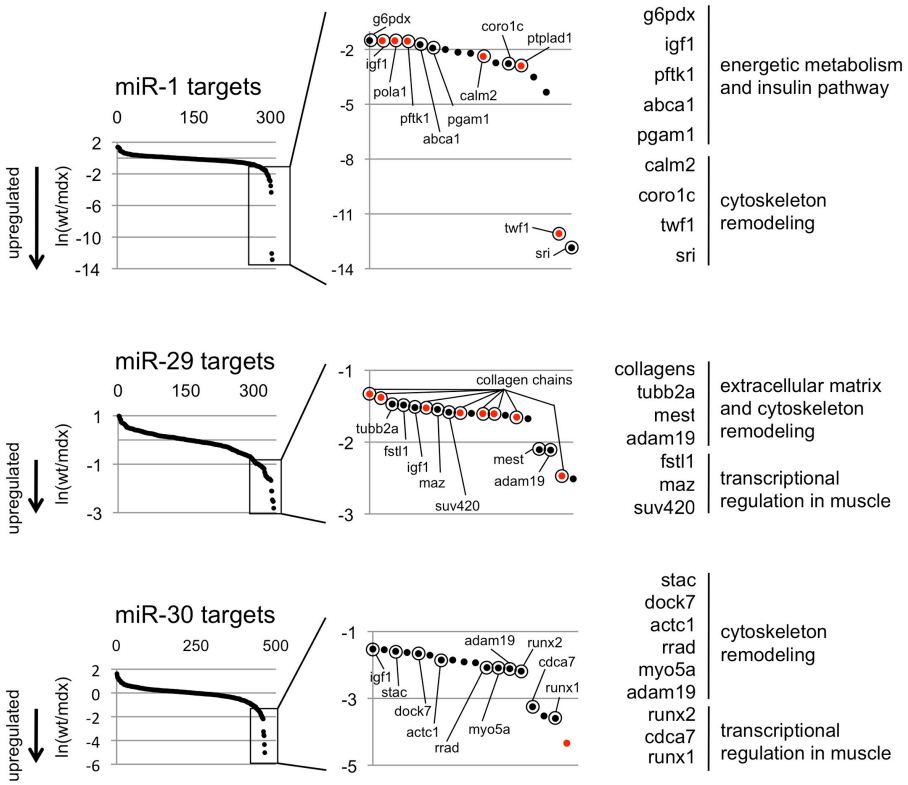
miR-1 targets
upregulated
ln(wt/mdx)
0
150
300
2
-2
-6
-10
-14
g6pdx
coro1c
ptplad1
igf1
pola1
calm2
pftk1
pgam1
abca1
twf1
sri
-2
-5
-8
-11
-14
g6pdx
igf1
pftk1
abca1
pgam1
energetic metabolism and insulin pathway
calm2
coro1c
twf1
sri
cytoskeleton remodeling
miR-29 targets
upregulated
ln(wt/mdx)
0
150
300
1
-1
-3
collagen chains
tubb2a
fstl1
igf1
maz
suv420
mest
adam19
-1
-2
-3
collagens
tubb2a
mest
adam19
extracellular matrix and cytoskeleton remodeling
fstl1
maz
suv420
transcriptional regulation in muscle
miR-30 targets
upregulated
ln(wt/mdx)
0
250
500
2
0
-2
-4
-6
adam19
runx2
cdca7
runx1
igf1
stac
dock7
actc1
rrad
myo5a
-1
-3
-5
stac
dock7
actc1
rrad
myo5a
adam19
cytoskeleton remodeling
runx2
cdca7
runx1
transcriptional regulation in muscle

Figure 10. Bioinformatics search for miRNA targets.
mRNA microarray expression data from wild type versus *mdx* mice (Tseng et al., 2002) were analyzed searching for those species to be predicted targets of the miRNAs responding to the Dys-nNOS pathway, which were shown to be down-regulated in *mdx*. An *ad hoc* algoritm based on Targetscan rules was employed. For each miRNA analyzed, the diagram shows the number of putative targets (x axis) versus the logarithm of wt/*mdx* values (y axis). The rectangles include the most up-regulated mRNAs; on the right panels, their list is shown selecting for those species that could be interesting for the Duchenne physiopathology (energetic metabolism, cytoskeleton remodelling, extracellular matrix, transcriptional regulation in muscle). Validated targets for the indicated miRNA are represented in red dots;

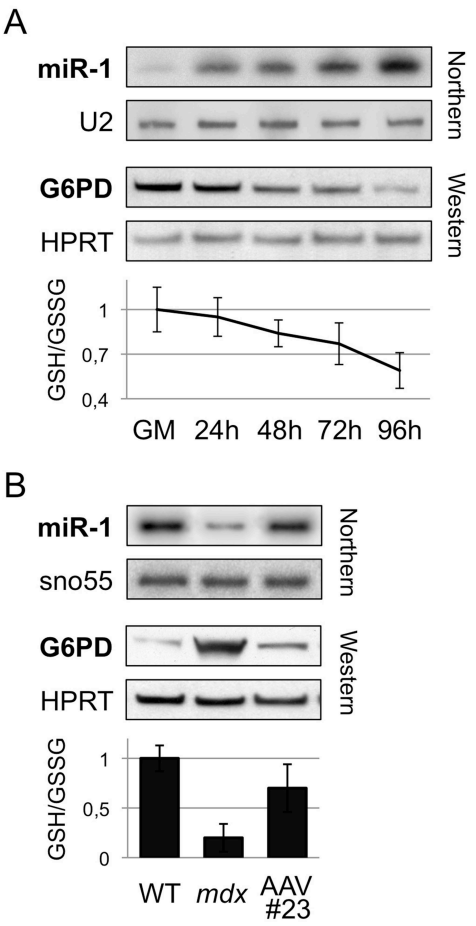

Figure 11. miR-1 controls G6PD expression.
(A) Total RNA and protein extracts, from C2 proliferating myoblasts (GM – growth medium) and after shift to differentiation medium (DM) for the indicated hours. Upper panels: Northern blot (miR-1 and U2 snRNA); middle panels: Western blot (G6PD and HPRT1); lower panel: GSH and GSSG ratio obtained by enzymatic assay titration. (B) Total RNA and protein extracts from WT, *mdx* and AAV#23-treated *mdx*. Upper panels: Northern blot (miR-1 and snoRNA55); middle panels: Western blot (G6PD and HPRT1); lower panel: GSH and GSSG ratio obtained by enzymatic assay titration. (C) Upper panel: protein extracts, from the gastrocnemius of control *mdx* (*mdx*) and *mdx* treated with G6PD (6-AN) or NOX (APO) inhibitors, were immunoprecipitated with antibodies against nitrosylated-Cys residues and analyzed for HDAC2 content by Western blot (nitroso-HDAC2). On the top of each lane the relative quantities (RQ) of nitroso-HDAC2 normalized for the amount of total cellular HDAC2, with *mdx* set to a value of 1, are indicated. Values are the average of three independent experiments. Lower panel: qRT-PCR for miR-1 on *mdx,* 6-AN and APO *mdx*-treated mice. Relative expressions were normalized to snoRNA55 and shown with respect to *mdx* set to a value of 1. (D) *mdx* animals were electroporated with a miR-1 expression construct (p-miR-1) in the right gastrocnemius or with an

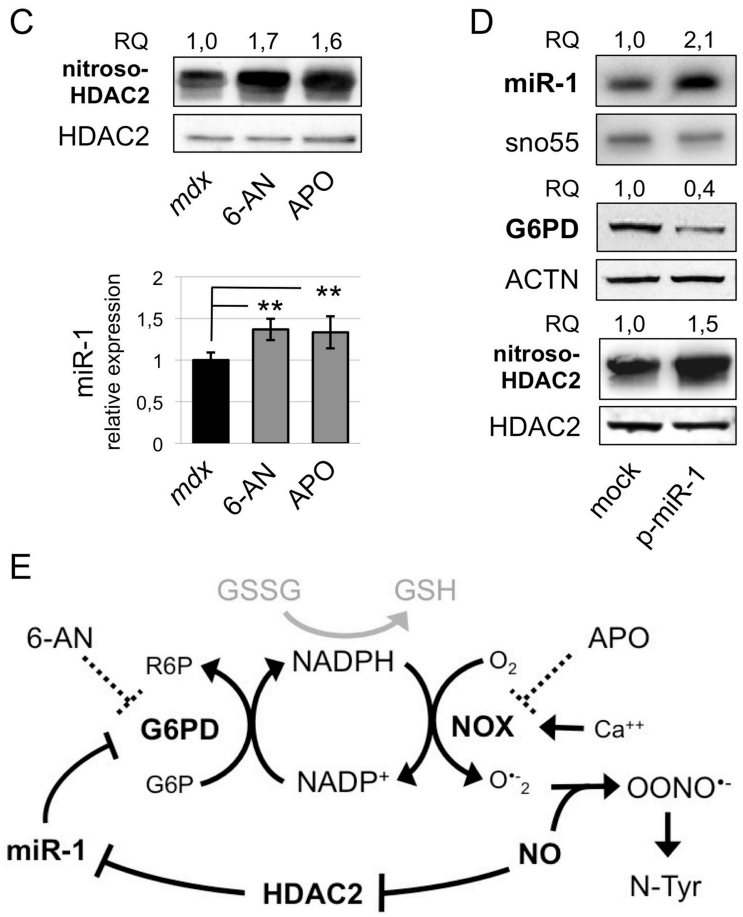

empty vector (mock) in the controlateral muscle and sacrificed after 25 days. miR-1, G6PD and nitroso-HDAC2 levels were measured. Relative quantities (RQ), shown with respect to *mdx* set to a value of 1, are indicated. The values are the average of three independent experiments. snoRNA55, ACTN and HDAC2 were used for normalization. (E) Pathway connecting G6PD, NOX, NO, HDAC2 and miR-1. Two asterisks ($p<0.01$).

miR-29 controls fibrosis in *mdx* muscles.
mdx animals undergo extensive fibrotic degeneration (Haslett et al., 2002). Crucial factors involved in this event are collagens and elastin, structural components of the extracellular matrix, whose mRNAs have been recently shown to be targeted by miR-29 family in myocardial infarction (van Rooij et al., 2008). qRT-PCR revealed that in *mdx,* where miR-29 is poorly expressed, the mRNAs for collagen (COL1A1) and elastin (ELN) were up-regulated. Their amount was instead reduced at levels similar to WT in AAV#23-treated animals, where miR-29 levels were resumed (Figure 12A). In order to test whether miR-29 alone is able to regulate collagen and elastin mRNAs in the Duchenne fibrotic process, we electroporated in the gastrocnemius of *mdx* animals a plasmid DNA containing an expression cassette driving the transcription of the miR-29a/b cluster (p-miR-29). Control *mdx* mice were electroporated with an empty plasmid. 25 days after treatment, muscles were dissected and the presence of p-miR-29 DNA was verified by PCR (Figure 12B). Northern blot indicated that a 2-3 fold over-expression of miR-29 was specifically obtained (Figure 12C) and that this paralleled a relevant decrease of collagen and elastin mRNAs (Figure 12D). Trichromic staining on *mdx* mice electroporated with p-miR-29 indicated a strong decrease in collagen deposition (blue stain) if compared to mock-electroporated muscles (Figure 12E). These data point to miR-29 as a crucial player in the control of the extracellular matrix modifications in *mdx* mice.

Figure 12. miR-29 controls fibrosis in *mdx*.
(A) qRT-PCR for collagen (COL1A1) and elastin (ELN) mRNAs performed on total RNA from the gastrocnemius of WT, *mdx* and AAV#23-treated *mdx* mice. Relative expressions were normalized to HPRT1 and shown with respect to WT set to a value of 1. In panels B-E the gastrocnemius of *mdx* animals were electroporated with a miR-29a/b expression construct (p-miR-29) and sacrificed after 25 days in parallel with WT and a control *mdx* electroporated with an empty plasmid (*mdx*). (B) PCR analysis on DNA from WT, *mdx* and p-miR-29 electroporated (1-4) *mdx*. Primers specific for the p-miR-29 construct and for the β-actin gene were utilized. (C) Northern blot for

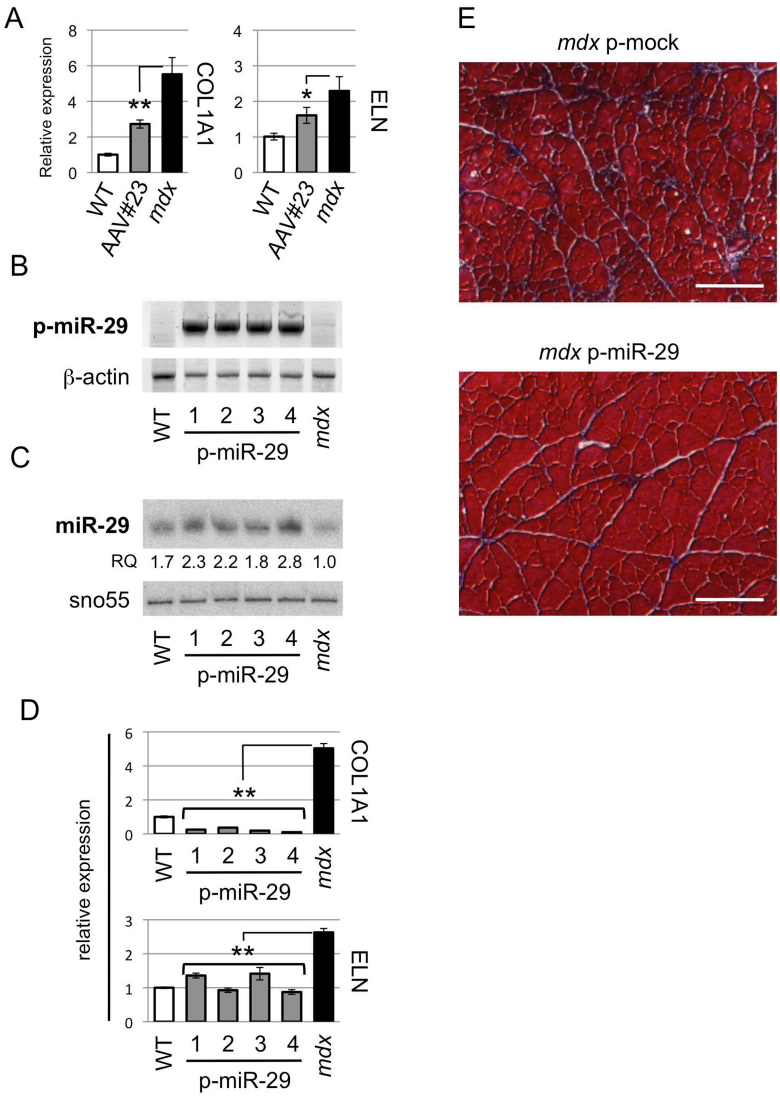

miR-29 and control snoRNA55. Relative quantities (RQ) of miR-29, relative to *mdx* set to a value of 1, are indicated below each lane. (D) qRT-PCR on COL1A1 and ELN mRNAs. Relative expressions are normalized to HPRT1 mRNA. Values are shown with respect to WT set to a value of 1. (E) Masson's trichrome staining indicates collagen deposition (blue stain) on p-mock and p-miR-29 electroporated *mdx*. Original magnification, X10. Scale bar 100 μm. One asterisk ($p<0.05$), two asterisks ($p<0.01$).

miR-31 and miR-206 are enriched in Duchenne muscles

miR-206 and miR-31 are highly enriched in *mdx* mice with respect to control while, as already shown, miR-1 decreases (Figure 13A). Their abundance correlated with degeneration and regeneration processes, since in muscles of 10 day-old *mdx*, before the onset of dystrophic symptoms, no up-regulation was observed (Figure 13B).
In *situ* hybridization (Figure 13C) showed that miR-206 and miR-31, almost absent in WT conditions, have a preferential co-localization in regenerating myoblasts $MyoD^{+}/MyoG^{+}/MHC^{-}$ (Figure 13D), identified by the characteristic phenotype of mononucleated fibers, highly abundant in *mdx*.

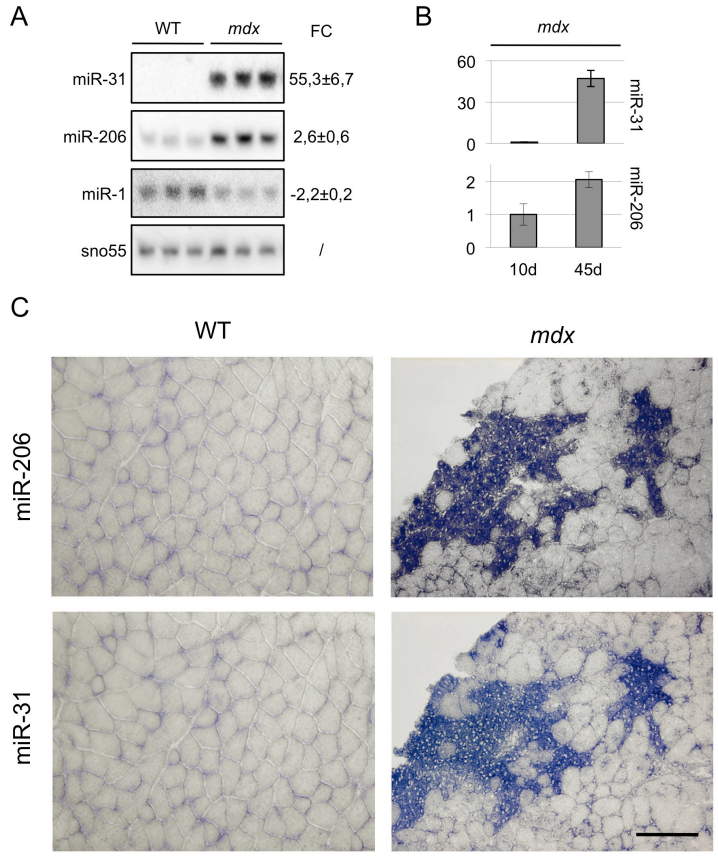

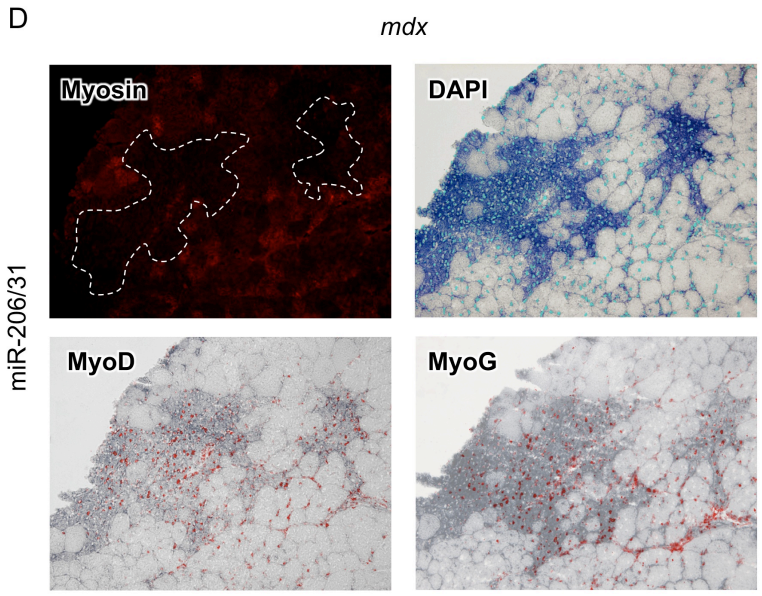

Figure 13. miR-206 and miR-31 are expressed in regenerating fibers.
(A) Representative Northern blot analysis for miR-31, miR-206 and miR-1 in three wild type (WT) and three *mdx* mice. snoRNA55 was used as a loading control. Fold changes are shown on the right (B) qRT-PCR for miR-31 and miR-206 in newborn (10d) and adult (45d) *mdx* mice. (C-D) Immunofluorescence and *in situ* analyses on wild type (WT) and mdx gastrocnemius serial sections with miR-31 and miR-206 DIG-labelled probes, DAPI and myosin, myoG and myoD antibodies. miR-31 and miR-206 positive regions lack myosin staining (see dashed regions in myosin panel). Original magnification X20, scale bar 100 μm.

miR-206 activates satellite cells differentiation through Pax7 repression

The differential behavior of miR-1 and miR-206 in WT versus *mdx* prompted us to analyze in more detail their pattern of expression. These miRNAs, while sharing the same seed, differs only for 4 nucleotides in the 3' portion. *In situ* hybridization analysis was performed on *mdx* and WT gastrocnemius by using DIG-labeled probes. Signals for miR-206 were restricted to immature regenerating fibers with centralized nuclei, whereas the miR-1 probe showed intense accumulation in mature differentiated fibers (Figure 14). Intact multi-nucleated fibers and small mononucleated cells, such as inflammatory cells, fibroblasts and proliferating satellite cells lacked the miR-206 signals (note the absence of signals in interstitial spaces). Therefore, increased expression of miR-206 in *mdx* muscles is due to differentiating satellite cells.
Next, we isolated mouse satellite cells from muscle biopses and differentiated them *in vitro* (Rando and Blau, 1994). miR-206 expression was activated at 12 hours and its accumulation proceeded during differentiation (Figure 15A, upper panel). Notably, the satellite-specifying factor Pax7 (Relaix et al., 2006), abundant in growth conditions, started to decrease at 12 hours and completely disappeared at 24 hrs, therefore showing an inverse correlation with miR-206 levels (Figure 15A, lower panel). Moreover, transfection of *in vitro* cultured satellite cells with anti-miR-206 LNA oligonucleotides indicated that in the absence of miR-206, Pax7 repression was unaffected at 12 hours and remained detectable up to 48 hours (Figure 15B). The link between Pax7 decrease, miR-206 induction and the presence of miR-206 putative target sites in the 3'UTR of Pax7 mRNA (Figure 15C) led us to study whether a regulatory interaction exists. Wild type Pax7 3'UTR and its mutant for miR-206 binding sites were cloned downstream Renilla ORF and reporter constructs were tranfected in C2 myoblasts. Luciferase assays show that reporter downregulation, in condition of miR-206 overexpression is achieved only on WT-3'UTR (Figure 15D). These experiments indicated that Pax7 can be repressed also by miR-1; however, as shown in the Northern of figure 15A, in cultured satellite cells miR-1 is almost undetectable at 12 hours when down-regulation of Pax7 starts, allowing to conclude that mainly mir-206 is expressed

at a time compatible with Pax7 repression. Therefore, these data demonstrates that miR-206 plays a specific role in early events of regeneration by repressing the activity of Pax7 thus allowing the progression of the differentiation program.
ChIP analysis for HDACs binding on the miR-1 and miR-206 loci in conditions of miRNA repression (GM - growth medium) versus miRNA activation (DM - differentiation medium) in C2 myoblasts indicated that, differently from miR-1, miR-206 is specifically repressed by HDAC1 (Figure 15E and F). The restricted expression of miR-206 in early phases of differentiation, before dystrophin synthesis starts, well correlates with its expression being unaffected by the Dys/nNOS/HDAC2 pathway.

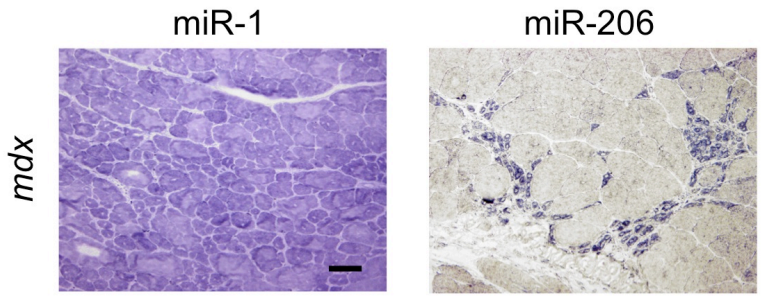

Figure 14. differential expression of miR-1 and miR-206. A miR-1 or miR-206 DIG-labelled probe was hybridized on *mdx* gastrocnemius sections. Original magnification, X20. Scale bar 50 μm.

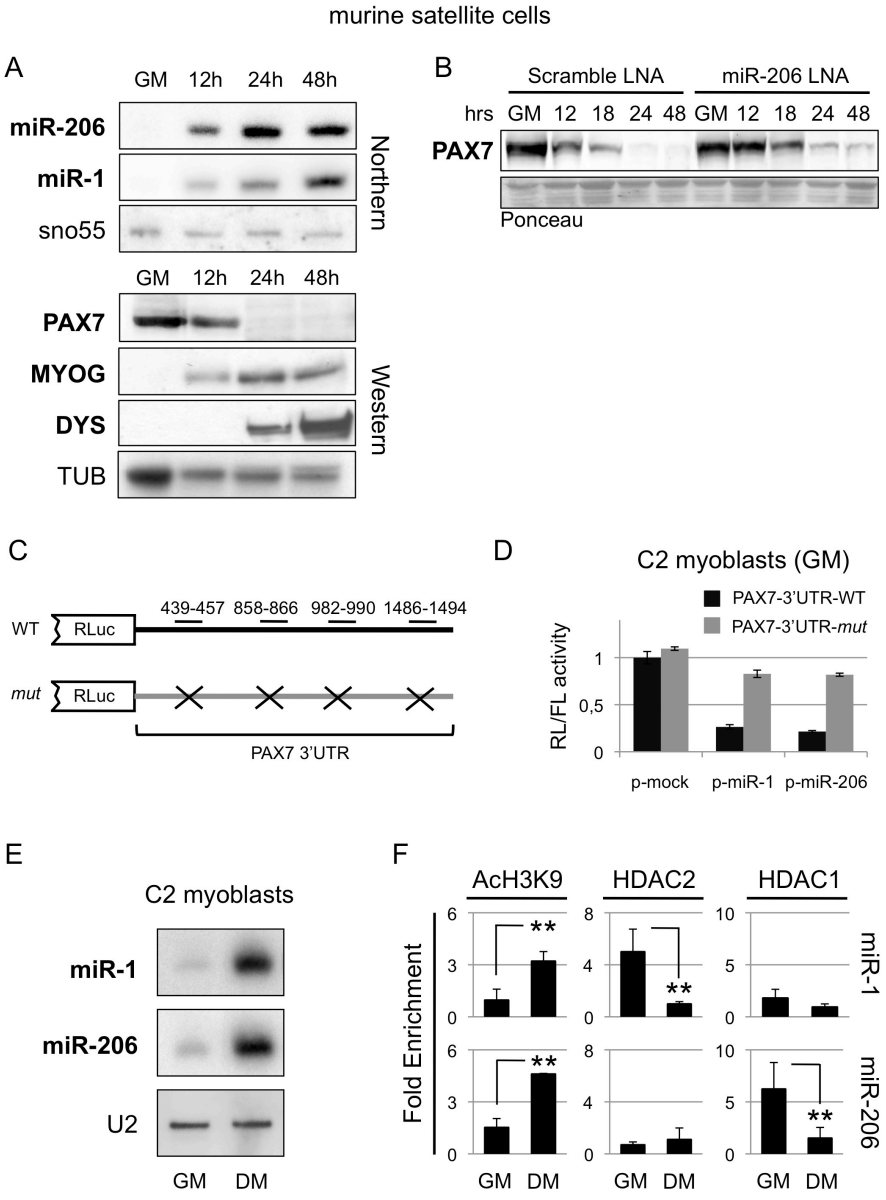
murine satellite cells
A
GM 12h 24h 48h
miR-206
miR-1
sno55
Northern
GM 12h 24h 48h
PAX7
MYOG
DYS
TUB
Western
B
Scramble LNA
miR-206 LNA
hrs GM 12 18 24 48 GM 12 18 24 48
PAX7
Ponceau
C
439-457 858-866 982-990 1486-1494
WT RLuc
mut RLuc
PAX7 3'UTR
D
C2 myoblasts (GM)
PAX7-3'UTR-WT
PAX7-3'UTR-mut
RL/FL activity
1
0,5
0
p-mock p-miR-1 p-miR-206
E
C2 myoblasts
miR-1
miR-206
U2
GM DM
F
AcH3K9
HDAC2
HDAC1
Fold Enrichment
6
3
0
8
4
0
10
5
0
**
miR-1
miR-206
GM DM GM DM GM DM

Figure 15. Pax7 is target of miR-206.
(A) RNA and protein samples were extracted from proliferating satellite cells (GM – growth medium) and after shift to differentiation medium (DM) for the indicated hours. Upper panels: Northern blots for miR-206, miR-1 and snoRNA55; lower panels: Western blots for PAX7, myogenin (MYOG), dystrophin (DYS) and tubulin (TUB). (B) Western blot for PAX7 on protein extracts of murine satellite cells transfected with anti-miR-206 or scramble LNA oligos in GM and switched to DM for the indicated hours. Ponceau staining was used as loading control. (C) Luciferase reporter with wild type (WT) Pax7 3'UTR or mutated for miR-206 target sites (D) Luciferase activity in C2 myoblasts in growth medium, in presence of miR-1 or miR-206 over-expression. (E) miR-1, miR-206 and U2 snRNA expression analyzed by Northern blot in C2 myoblasts maintained in GM or in DM for 5 days. (F) ChIP analysis on miR-1-2/133a and miR-206 promoters with antibodies against AcH3K9, HDAC2 and HDAC1 on chromatin from C2 cells in GM and DM. 5,8S rDNA was used as internal negative control. Results are expressed as fold-enrichment of DNA immunoprecipitated samples relative to INPUT chromatin. Two asterisks ($p<0.01$).

miR-31 is expressed in DMD myoblasts delayed in differentiation

Also in human DMD biopsies, miR-31 was more abundant if compared to healthy and Becker muscles (Figure 16A). miR-31 remained high in DMD myoblasts induced to differentiate *in vitro,* whereas in human healthy controls its levels decreased with progression of differentiation (Figure 16B). DMD myoblasts appeared to have a higher proliferating capacity and a lower differentiation potential than control cells. This was shown by the presence of PAX7 in growth conditions and by the delayed appearance of differentiation markers upon serum withdrawal (Figure 16C). In control myoblasts, myogenin peaked already at day 2 of differentiation, preceding myosin heavy chain and dystrophin synthesis; whereas in DMD cells, myogenin appeared only at day 4 preceding MHC synthesis, clearly visible at day 6. Immunostaining of the same samples confirmed that DMD cells express MHC protein at lower levels and later than Ctrl cells (Figure 16C and D).
These data, together with results in Figure 13 indicate that the high levels of miR-31 in Duchenne muscles is due on one side to intensive regeneration involving activated satellite cells and on the other to the reduced ability of Duchenne myoblasts to complete the differentiation programme.

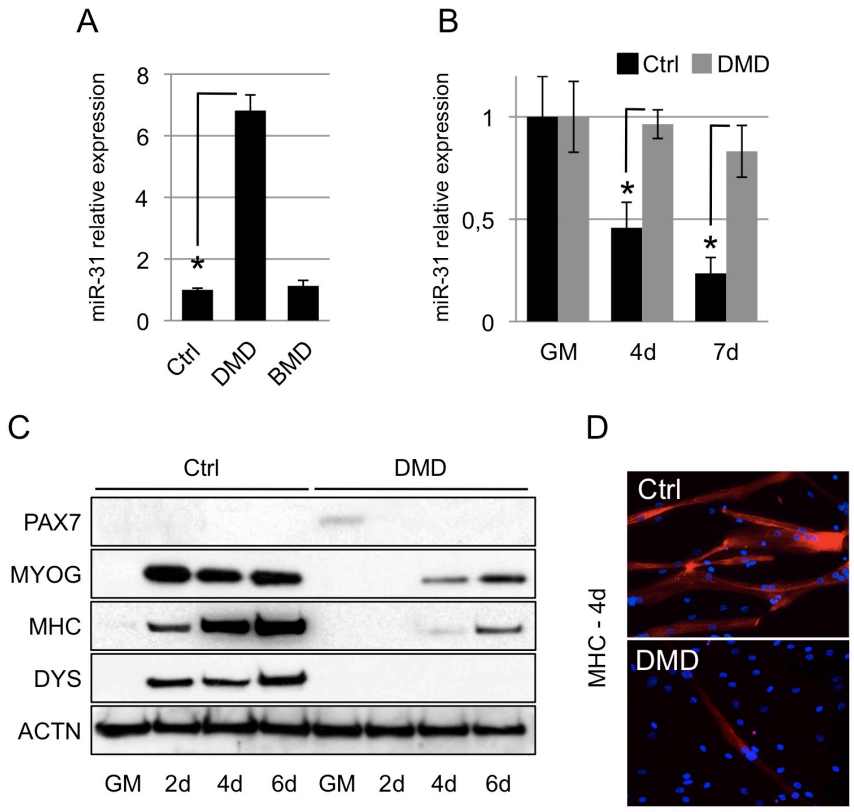

Figure 16. miR-31 is expressed in delayed DMD myoblasts. (A) qRT-PCR of miR-31 relative expression in human muscle biopsies from healthy (Ctrl), Duchenne (DMD) and Becker (BMD) donors. (B) qRT-PCR of miR-31 relative expression in human primary myoblasts from healthy donors (Ctrl, black bars) or DMD patients (DMD, grey bars) in growth medium (GM) and at the indicated time points after shift to differentiation medium. (C) The same cells were analyzed by Western blot for PAX7, myogenin (MyoG), Myosin Heavy Chain (MHC) and Dystrophin (DYS). Actinin (ACTN) was used as a loading control. The values are derived from at least three independent experiments. Asterisks: $p<0.05$. (D) Immunofluorescence staining with MHC antibodies (red) and DAPI (blue) on Ctrl and DMD myoblasts at 4 days after induction of differentiation.

miR-31 targets dystrophin mRNA

In silico analysis, performed by comparing mRNA expression profiles in wild type versus *mdx* animals (data not shown), identified a large number of predicted targets of miR-31. Notably, the most down-regulated mRNA in *mdx* muscles encode for proteins involved in terminal differentiation, including dystrophin. One putative binding site, embedded in a 40 nucleotide region perfectly conserved among mammalian species, was identified in the 3'UTR of the dystrophin mRNA (Figure 17A). Wild type dystrophin 3'UTR (DMD-WT) and a derivative mutated in the miR-31 target site (DMD-*mut*) were fused to the luciferase ORF (Figure 17B). Enzyme activity was measured in C2 myoblasts in endogenous conditions and upon miR-31 overexpression (Figure 17C). The results indicate that miR-31 repressed luciferase activity only on DMD-WT and that de-repression was obtained with LNA oligos against miR-31 and not with control scramble LNA. Scramble LNA transfection *per se* did not affect luciferase activities (not shown). Moreover, when cells were treated with a sponge-construct containing four binding sites for miR-31 (Sponge-31, Figure 17A and B), luciferase activity resulted higher with respect to cells treated with a control construct (Figure 17D). Release from miR-31 repressing activity was also obtained when cells were treated with a LNA oligo complementary to 23 nucleotides across the miR-31 target site (protector-31) both in the presence of the endogenous miR-31 and in conditions of miR-31 overexpression (Figure 17E).
These data indicate that miR-31 targets the 3'UTR of the dystrophin mRNA and that repression is prevented either by the use of miR-31 decoys or by protecting the miR-31 binding site on dystrophin mRNA.

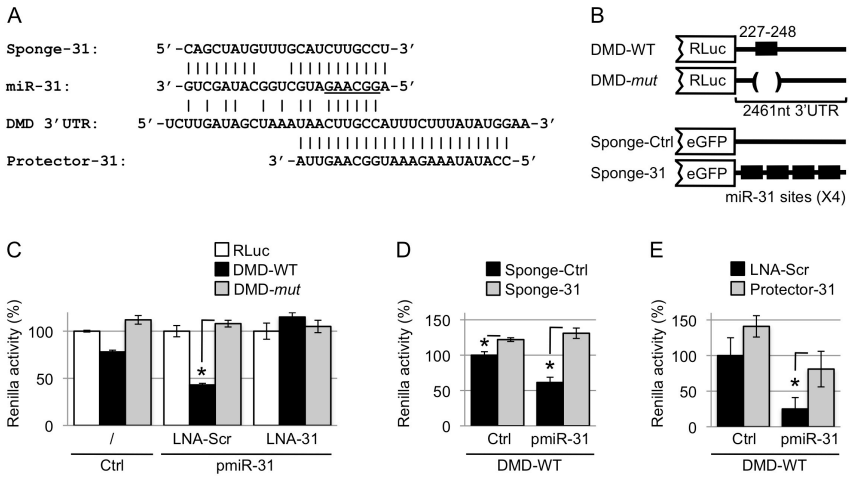

Figure 17. miR-31 targets Dystrophin mRNA.
(A) Sequences of: the mature miR-31, the conserved 40 nucleotide region of the DMD 3'UTR, the decoy sequence of the sponge-31 construct and the 23 nucleotide LNA protector (Protector-31) covering miR-31 binding site on the DMD 3'UTR. miR-31 seed sequence is underlined. (B) Schematic representation of: the luciferase constructs containing the wild type 3'UTR of the dystrophin mRNA (DMD-WT) and its mutant derivative with a deletion of the miR-31 target site (DMD-*mut*), the sponge constructs containing the GFP gene with a control 3'UTR (Sponge-Ctrl) or with the same 3'UTR containing four miR-31 decoy sites (Sponge-31). (C) Renilla Luciferase activity in proliferating C2 myoblasts transfected with the control Rluc vector or DMD-WT or DMD-*mut.* in combination with the plasmid overexpressing miR-31 (pmiR-31) or a control plasmid (Ctrl). Cells were also transfected with control (LNA-Scr) or anti-miR-31 (LNA-31) LNA oligos. Renilla activity of the Rluc vector was set to a value of 100% in all treatments. (D) Renilla Luciferase activity in C2 myoblasts transfected with DMD-WT, in the presence of Sponge-Ctrl or Sponge-31 constructs, with pmiR-31, or a control plasmid. (E) Renilla Luciferase activity in C2 myoblasts transfected with DMD-WT alone (Ctrl) or upon miR-31 overexpression (pmiR-31) in the presence of control (LNA-Scr) or protector (Protector-31) LNAs. The values of all experiments are derived from at least three independent experiments. Asterisks: $p<0.05$.

miR-31 inhibition enhances exon skipping treatment

In vitro differentiation of C2 mouse myoblasts indicated that miR-31 was expressed at good levels in proliferating conditions (GM) and its levels decreased upon differentiation (Figure 18A). Synthesis of dystrophin was prominent only at day 5 even though transcription was already consolidated at day 3. These data reflected the expected inverse correlation between the miRNA and its putative target. We next tested in C2 myoblasts whether the endogenous synthesis of dystrophin correlated to altered levels of miR-31 (Figure 18B): overexpression was obtained through infection with a lentivirus containing the pri-miR-31 expression cassette (miR-31), while depletion was obtained via administration of LNA-31 or sponge-31. When cells were induced to differentiate, a consistent decrease of dystrophin (almost 3-fold) was observed in conditions of persistent overexpression of miR-31; on the contrary, increase in dystrophin levels was detected when cells were treated with LNA-31 or sponge-31. In the last two cases, the limited increase (50 and 40% respectively) of dystrophin synthesis is likely due to the fact that miR-31 levels already start to decrease at 3 days of differentiation (Figure 18A). In the lower panels of Figure 18B the levels of the dystrophin protein are compared with those of its mRNA; in all cases dystrophin mRNA levels were not affected by miR-31 modulation, indicating that the miRNA acts by repressing translation rather than controlling dystrophin mRNA stability.
DMD myoblasts, from patient with deletion of exons 48-50, were infected with the U1#51 construct able to induce skipping of exon 51 and to rescue dystrophin synthesis (Figure 18C and D; Incitti et al., 2010). In order to check whether dystrophin synthesis could be further improved by reducing miR-31 levels, we tested the ability of the sponge-31 construct to increase dystrophin levels when infected in Δ48-50 DMD myoblasts. Figure 18D shows that sponge construct was indeed able to increase by 3-fold dystrophin synthesis when exon skipping was applied to these cells. Moreover, also the anti-miR-31 LNA oligos were able to increase dystrophin synthesis (2-fold) when transfected into exon skipping-treated cells. qRT-PCR showed that dystrophin mRNA levels were the same in the different conditions, similarly to the MCK mRNA.

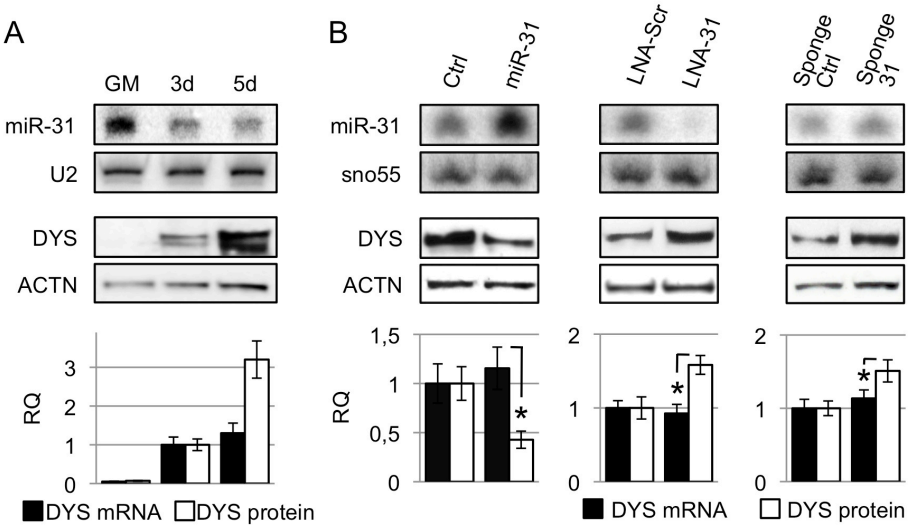

Figure 18. Effects of miR-31 modulation on dystrophin expression. (A) Northern (miR-31 and U2) and Western (DYS and ACTN) analyses of C2 mouse myoblasts in growth medium (GM) and at 3 and 5 days after shift to differentiation medium. The histogram at the bottom shows the relative quantification (RQ) of dystrophin protein and mRNA levels referred to the 3 day point set to a value of 1. (B) Northern (miR-31 and sno55) and Western (DYS and ACTN) analyses on C2 myoblasts treated with: lentiviruses with control (Ctrl) or miR-31 (miR-31) expression cassettes, control (LNA-Scr) or anti-miR-31 (LNA-31) LNA oligos and lentiviruses carrying Sponge-Ctrl or Sponge-31. Differentiation was allowed to proceed for 3 days. Dystrophin mRNA (DYS mRNA, black bars) and protein (DYS protein, white bars) levels were measured from three independent experiments. Histograms at the bottom show the relative quantifications (RQ) of dystrophin protein and mRNA levels referred to the values of control experiments (Ctrl, LNA-Scr and Sponge-Ctrl) set to 1.

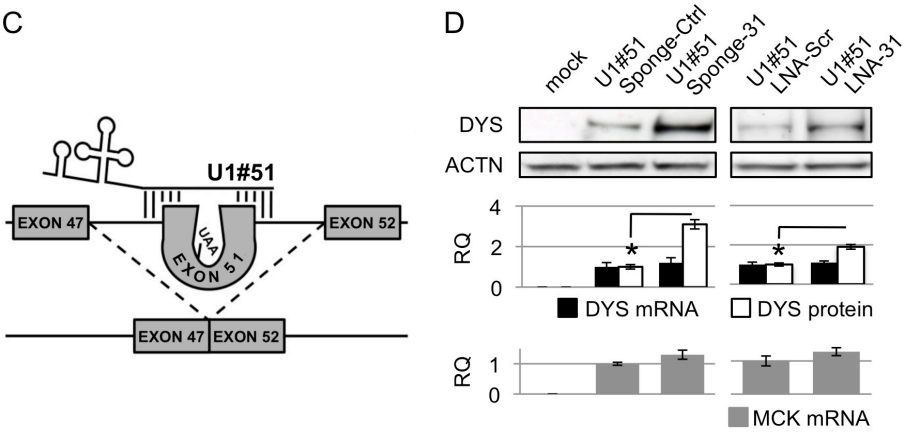

(C) Schematic representation of the exon skipping strategy for the human Δ48-50 DMD mutation. (D) human Δ48-50 DMD myoblasts were infected with control (mock) or U1#51 lentiviruses alone or in combination with the miR-31 sponge (U1#51 Sponge-31). Alternatively, cells treated with the exon skipping construct (U1#51) were transfected with control (LNA-Scr) or anti-miR-31 (LNA-31) LNA oligos. Cells were induced to differentiate for 5 days and dystrophin quantified by Western blot. Histograms show the RQ of dystrophin protein and mRNA levels as well as MCK mRNA levels respectively referred to the values of control experiments set to 1. Asterisks: $p<0.05$.

DISCUSSION

In Duchenne Muscular Dystrophy, muscle fiber breakage and degeneration, due to the absence of dystrophin, are accompanied by a complex series of events including activation of satellite cells, inflammatory infiltration, intense fibrosis and oxidative stress. These pathogenetic features are ameliorated in *mdx* mice in which dystrophin is rescued through different therapeutic strategies (Aartsma-Rus et al., 2009). Surprisingly, the beneficial effects observed on muscle function and morphology could be obtained also with low levels of rescued protein (Denti et al. 2008; Ghahramani Seno et al., 2008), suggesting that partial protein re-localization to the membrane could be only part of the story. Dystrophin has been suggested to affect gene expression through activation of the NO pathway and HDAC2 regulation (Colussi et al., 2009); however, no specific genes and regulatory circuitries that could account for the observed morpho-functional benefits had been characterized. In this work, taking advantage of the exon skipping strategy, we identified a specific group of miRNAs whose expression depends on dystrophin levels and whose de-regulation explains several DMD pathogenetic traits. This class of miRNAs, poorly expressed in *mdx*, was up-regulated in exon skipping-treated animals and included muscle specific (miR-1 and miR-133) and more ubiquitous (miR-29 and miR-30) ones. The same miRNAs displayed a dystrophin-dependent up-regulation also in human DMD myoblasts rescued for dystrophin synthesis through exon skipping.

The transcriptional activation of these miRNAs correlated with the acetylation state of H3K9 and modulation of HDAC2 binding to their promoters: in absence of dystrophin, the low miRNA expression levels paralleled persistence of HDAC2 onto miRNA regulatory regions. On the contrary, when dystrophin synthesis was rescued, HDAC2 was released from miRNA promoters and their transcription resumed. The use of mutated HDAC2 as well as treatment of *mdx* mice with NO-donors (NTG) indicated that the release of HDAC2 from chromatin was due to its nitrosylation. Notably, we showed that as a consequence of dystrophin rescue, nNOS was stabilized and re-localized on the muscle membrane and this directly affected the nitrosylation levels of HDAC2. Altogether, these data allowed us to conclude that Dystrophin, nNOS, HDAC2 nitrosylation and miRNAs

are on the same regulatory pathway as indicated in the model of Figure 19.
Analysis of the targets of the modulated miRNAs underscored regulatory networks important for understanding the DMD physiopathology. One relevant discovery was the finding that miR-1 controls the Glucose 6-Phosphate Dehydrogenase (G6PD), an housekeeping enzyme encoded in mammals by an X-linked gene. G6PD has important functions in intermediary metabolism because it catalyzes the first step in the pentose phosphate pathway and provides reductive potential in the form of NADPH; in fact, through NADPH production, G6PD is required to maintain cytosolic GSH levels and to protect against free radical injury. Disruption of the G6PD gene in male mouse embryonic stem cells indicated that G6PD activity is dispensable for pentose synthesis, but is essential to protect cells against even mild oxidative stress (Pandolfi et al., 1995). At variance with normal muscles, in degenerating fibers most of the NADPH produced is utilized in the O_2 to $O^{\circ-}_2$ conversion mediated by the Ca^{++}-dependent activation of NADPH oxidase (NOX; Gupte et al., 2006; Shkryl et al., 2009), suggesting that in dystrophic fibers G6PD may have an aberrant action in radical production. Indeed, in *mdx* fibers higher expression levels of NADPH oxidase were detected (Shkryl et al., 2009), suggesting a major contribution of this enzyme to the well documented oxidative stress occurring in these damaged muscles. Moreover, dystrophin-deficient cells were shown to be more susceptible to free radical induced injury if compared to normal cells, even though the two populations were equally susceptible to other forms of metabolic stress (Rando et al., 1998).
In line with these data, we demonstrated that while miR-1 was able to down-regulate G6PD, decreasing the levels of GSH in normal muscles, in dystrophic ones the increase in G6PD did not correlate with GSH levels. In *mdx* muscles, where the NADPH oxidase (NOX) undergoes up-regulation, most of the NO pool is utilized to convert superoxide species ($O^{\circ-}_2$) into peroxinitrite ($ONOO^-$); indeed we show that under these conditions HDAC2 is poorly nitrosylated, paralleling miR-1 repression and G6PD up-regulation. Exogenous modulation of this pathway, through G6PD or NOX inhibition, had consequent effects both in increasing HDAC2 nitrosylation and miR-1 up-regulation. Finally, local over-expression of miR-1 in *mdx* muscles determined down-regulation of G6PD and in turn increase of HDAC2

nitrosylation. Altogether these data proved the existence of a feed forward circuitry between G6PD and miR-1 through nitrosylation of HDAC2 (Figure 11E) and suggested that the regulatory network dependent on the dys/nNOS pathway has physiological relevance in controlling also the oxido-reductase state of the injured muscle.
The relevant role of the identified dystrophin-dependent miRNAs in the DMD pathogenesis was also tested for mir-29. Its over-expression in the gastrocnemius of *mdx* animals indicated that not only the target mRNAs for collagen and elastin were specifically down-regulated, but also that the muscles recovered a phenotype with a strong reduction in fibrosis.
These findings show a new link between the dystrophin/nNOS pathway and important molecular circuitries, including specific miRNAs and their targets, which play an important role in muscle differentiation, homeostasis and integrity (Figure 19).

At variance with the other myomiRs, mainly present in mature fibers, miR-206 and miR-31 were restricted to differentiating satellite cells; therefore, their higher levels in *mdx* and exon skipping-treated animals were due to massive regeneration occurring in dystrophic muscles. The compartmentalized expression observed *in vivo* was confirmed in cultured satellite cells where miR-206 was shown to repress Pax7. This transcriptional factor, which is the mark of myogenic progenitor cells, has been described to regulate self-renewal of satellite cells and their entry into the program of skeletal muscle differentiation (Figure 20; Buckingham and Relaix, 2007).
Moreover, miR-206 differed from miR-1, also because it was shown to be under the HDAC1 control. This, together with the restricted expression in activated satellite cells before the onset of dystrophin synthesis, is consistent with the finding that miR-206 is independent from the dys/nNOS pathway active in mature differentiated fibers. These data disclose a different function for the two members of the miR-1 family and provide a molecular mechanism for understanding how the switch between proliferation and differentiation of satellite cells can be obtained.

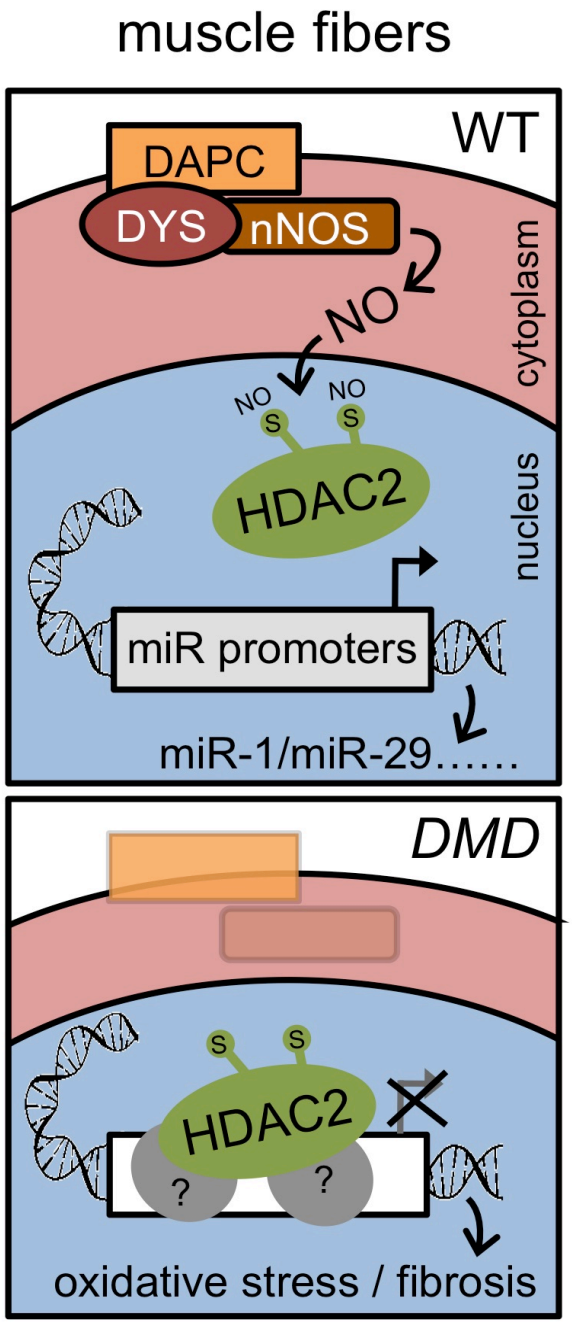

Figure 19. Model of the pathway connecting dystrophin to specific miRNA genes.
In WT muscle fibers the dystrophin-DAPC complex activates nNOS and S-nitrosylation of HDAC2. The modified HDAC2 is released from chromatin and activation of a specific subset of miRNA occurs. In Duchenne Muscular Dystrophy this circuitry is deregulated due to impaired nNOS activity and decrease in HDAC2 nitrosylation causing its retention to miRNA promoters.

The differential regulation of miR-1 and miR-206 also suggests that the epigenetic control mediated by the late differentiation marker, dystrophin, is important for increasing the robustness of the muscle differentiation programme consolidating the expression of those miRNAs involved in circuitries of terminal differentiation and tissue integrity.

In line with this, we described miR-31 as part of circuitries controlling late muscle differentiation by repressing dystrophin synthesis and, likely, many other terminal differentiation markers. miR-31 was previously described to repress myf5, a key element of muscle differentiation, both in muscle and brain (Daubas et al., 2009).
miR-31 repressing activity was detected in early phases of myoblasts differentiation supporting the idea that this control is necessary in normal muscle cells to avoid early expression of late differentiation markers and, specifically, dystrophin.
The intense and localized expression of miR-31 in regenerating myoblasts of dystrophic muscles indicated that the high levels of miR-31 found in dystrophic conditions (both in mouse and human biopsies) are due to the intensive regeneration program which is mediated by the activation of satellite cells. Interestingly, in dystrophic myoblasts and satellite cells the lack of dystrophin correlated with a delay of the maturation process of the cells.
In this study we have also shown that in dystrophic conditions, when dystrophin synthesis is rescued through the exon skipping strategy, the inhibition of miR-31 activity increased dystrophin production. Since in a compromised muscle the contribution to dystrophin production by regenerating fibers is quite relevant, miR-31 repression in this compartment can represent an improvement to current therapeutic treatments aimed to increase the levels of dystrophin synthesis. Rescue of consistent levels of dystrophin will also have additional benefits such as the completion of the muscle fiber maturation process (Figure 20).

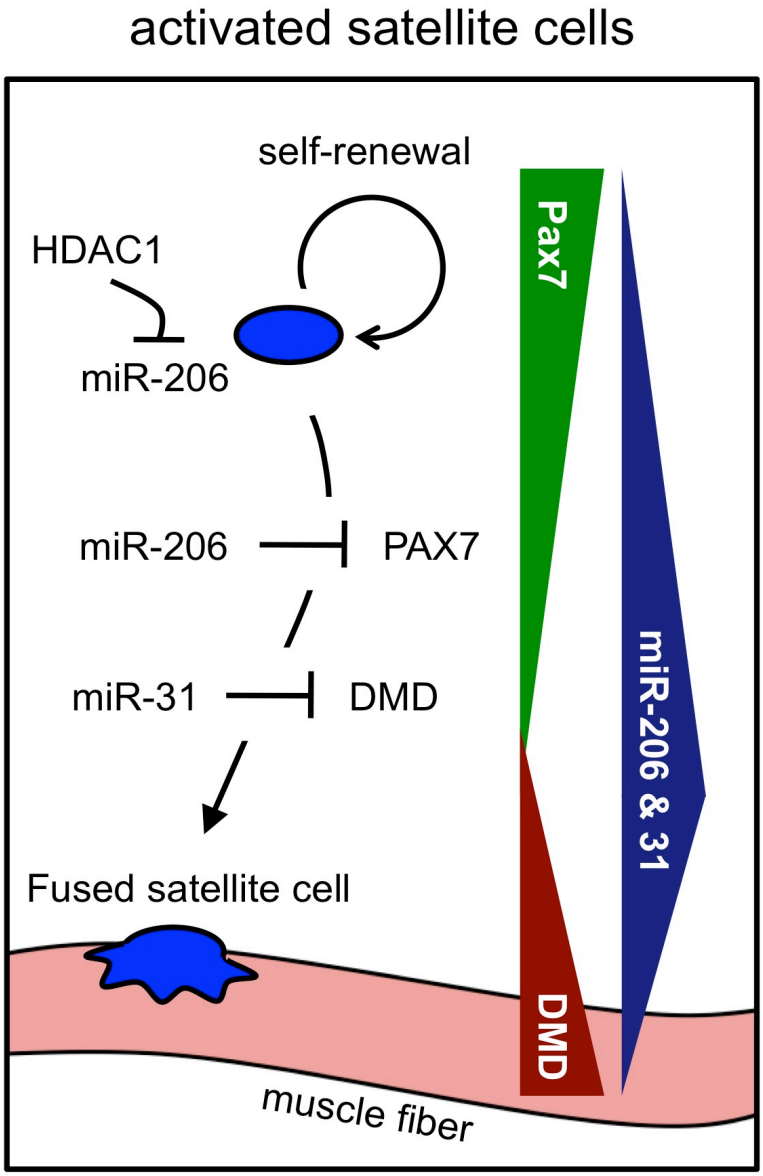

Figure 20. miR-206 and miR-31 regulate muscle regeneration. miR-206 and miR-31 are expressed in differentiating satellite cells where miR-206 represses Pax7 allowing differentiation to proceed and miR-31 inhibits dystrophin avoiding its early expression.

MATERIALS AND METHODS

Animal treatments and constructs. 6 week-old *mdx* mice were tail vein injected with 0.5-1x10^{12} genome copies of the AAV-U1#23 (AAV#23) or virus as described in Denti et al. (2006) and sacrificed after 4 weeks. Electroporation was performed on 6 week-old *mdx* as described in Donà et al. (2003). Wild type and mutant FLAG-HDAC2 plasmids provided by Dr A. Riccio and described in Nott et al. (2008). Nitroglycerin treatments were performed on 6-18 weeks-old *mdx* mice by local injections of 0,3 mg/kg of nitroglycerin or physiological solution in tibialis or gastrocnemius muscles and sacrificed after 4 hours. Apocynin and 6-aminonicotinamide were administered to *mdx* mice by osmotic pumps (ALZET) as in Walker et al. (1999) and Gupte et al. (2006).

Cell culture. Muscle satellite cells were cultured and differentiated as described in Rando and Blau (1994). The Duchenne primary myoblasts carrying exons 48-50 deletion were obtained from Telethon Biobank (Carlo Besta Institute, Milan), and infected with a lentiviral construct containing antisense sequences against the splice junctions of exon 51 (LV#51, Incitti et al, 2010). LNA miRNA Knockdown (Exiqon) treatment were performed according to Taulli et al. (2009).

Protein and miRNA in situ analyses. Western blot on total extracts, H&E staining and *in situ* analyses on 7 μm-thick gastrocnemius cryosections were performed as described in Denti et al. (2006). *In situ* hybridizations were performed with NCL-DYS2 (Novocastra), nNOS, myoD, myoG, MHC (Santa Cruz). Immunoprecipitations on protein extracts were performed with antibody against S-nitroso-Cys (Sigma) according to manufacturer's specifications and revealed by Western blot using an antibody against HDAC2 (Upstate). Masson's Trichrome staining (Sigma) was performed according to manufacturer's specifications. miRNA in situ hybridization was performed in formaldehyde and EDC-fixed gastrocnemius cryosections according to Pena et al. (2009).

Chromatin immunoprecipitation assays. ChIP analysis was performed according to Ballarino et al., (2005) with the following antibodies: HDAC2 and RNA Pol II (Santa Cruz), HDAC1, HDAC4, acetylated H3-Lys9 (Upstate) and FLAG (Sigma). The starting material was 1-3mm^3 for tissue samples or 1-10x10^5 cultured cells.

ChIP assays on DMD cells were performed using the EZ Magna ChIP Assay Kit (Millipore) following manufacturer's specifications.

RNA preparation and analysis. Total RNA was prepared from liquid nitrogen powdered tissues homogenized in Qiazol reagent (QIAGEN). miRNA and mRNA analyses were performed using miScript System (QIAGEN). Relative quantification was performed using as endogenous controls U6 snRNA for miRNAs and HPRT1 for mRNAs. Northern blots for miRNAs were performed using LNA detection probes (Exiqon).

Luciferase constructs and assays. Full length murine 3'UTR sequences of G6PD, PAX7 and DMD were amplified by PCR and then cloned in *Not I* restriction site of the psicheck2 plasmid (Promega), downstream the renilla luciferase (RLuc) gene. The same plasmid contains also the firefly luciferase (FLuc) to normalize transfection efficiency. Mutant derivative were obtained by deletion of miRNA binding sites by inverse PCR. RLuc and FLuc activities were measured by Dual Glo luciferase assay (Promega).

GSH/GSSG. GSH and GSSG titration were performed by fluorimetric assays (Biovision) according to manufacturer's specifications.

miRNA overexpression and sponge constructs. miRNA overexpression constructs were produced by cloning pri-miRNA sequences, with 100 nucleotides upstream and downstream the pre-miRNA, into the U1snRNA expression cassette (according to Denti et al., 2004). Sponge-31 construct was generated by cloning annealed oligonucleotides containing four miR-31 artificial binding sites into the WPRE *SacII* restriction site downstream the GFP open reading frame according to Gentner et al. 2009. miR-31 sponge was combined with exon skipping by cloning annealed oligos into the WPRE sequence of GFP reporter of lentiviral PCCL-U1#51 reported to induce skipping of DMD exon 51 (Incitti et al., 2010).

Statistical analyses. Each data shown in histograms is the result of at least three independent experiments performed on at least three different samples/animals. Data are shown as mean ± standard deviation. Unless specifically stated, statistical significance of differences between means was assessed by two-tailed t-test and a $p < 0.05$ was considered significant.

ACKNOWLEDGMENTS

I would like to thank the other authors Dr. Martone Julie, Dr. Cesana Marcella, Dr. Incitti Tania, Dr. Girardi Erika, Dr. Morlando Mariangela, Dr. Nicoletti Carmine, Dr. Santini Tiziana, Dr. Sthandier Olga, Dr. Barberi Laura, Prof. Auricchio Alberto, Prof. Musarò Antonio and Prof. Bozzoni Irene.
I would like also to thank Dr. E. Bertini, Dr A. D'Amico, Dr. M. Mora, Prof. A. Riccio, Prof. P. Paggi, Dr. L. Lombardi and the Telethon Neuromuscular Biobank for providing material. We also thank M. Marchioni for technical support. DC is a recipient of a Microsoft research PhD fellowship. This work was partially supported by grants from: Telethon (GGP07049), Parent Project Italia, EU project SIROCCO (LSHG-CT-2006-037900), ESF project "NuRNASu", IIT "SEED", PRIN and BEMM.

REFERENCES

- Aartsma-Rus A, Van Deutekom JC, Fokkema IF, Van Ommen GJ, Den Dunnen JT. Entries in the Leiden Duchenne muscular dystrophy mutation database: an overview of mutation types and paradoxical cases that confirm the reading-frame rule. Muscle Nerve. 2006 Aug; 34 (2) :135-44.
- Aartsma-Rus A, Fokkema I, Verschuuren J, Ginjaar I, van Deutekom J, van Ommen GJ, den Dunnen JT. Theoretic applicability of antisense-mediated exon skipping for Duchenne muscular dystrophy mutations. Hum Mutat. 2009 Mar; 30 (3) :293-9.
- Athanasopoulos T, Graham IR, Foster H, Dickson G. Recombinant adeno-associated viral (rAAV) vectors as therapeutic tools for Duchenne muscular dystrophy (DMD). Gene Ther. 2004 Oct; 11 Suppl 1:S109-21.
- Ballarino M, Pagano F, Girardi E, Morlando M, Cacchiarelli D, Marchioni M, Proudfoot NJ, Bozzoni I. Coupled RNA processing and transcription of intergenic primary microRNAs. Mol Cell Biol. 2009 Oct; 29 (20) :5632-8.
- Brenman JE, Chao DS, Xia H, Aldape K, Bredt DS. Nitric oxide synthase complexed with dystrophin and absent from skeletal muscle sarcolemma in Duchenne muscular dystrophy. Cell. 1995 Sep 8; 82 (5) :743-52.
- Buckingham M, Relaix F. The role of Pax genes in the development of tissues and organs: Pax3 and Pax7 regulate muscle progenitor cell functions. Annu Rev Cell Dev Biol. 2007; 23:645-73.
- Chen JF, Mandel EM, Thomson JM, Wu Q, Callis TE, Hammond SM, Conlon FL, Wang DZ. The role of microRNA-1 and microRNA-133 in skeletal muscle proliferation and differentiation. Nat Genet. 2006 Feb; 38 (2) :228-33.
- Colussi C, Illi B, Rosati J, Spallotta F, Farsetti A, Grasselli A, Mai A, Capogrossi MC, Gaetano C. Histone deacetylase inhibitors: keeping momentum for neuromuscular and cardiovascular diseases treatment. Pharmacol Res. 2010 Jul; 62 (1) :3-10.
- Colussi C, Gurtner A, Rosati J, Illi B, Ragone G, Piaggio G, Moggio M, Lamperti C, D'Angelo G, Clementi E, Minetti G, Mozzetta C, Antonini A, Capogrossi MC, Puri PL, Gaetano C. Nitric oxide

deficiency determines global chromatin changes in Duchenne muscular dystrophy. FASEB J. 2009 Jul; 23 (7) :2131-41.
• Colussi C, Mozzetta C, Gurtner A, Illi B, Rosati J, Straino S, Ragone G, Pescatori M, Zaccagnini G, Antonini A, Minetti G, Martelli F, Piaggio G, Gallinari P, Steinkuhler C, Clementi E, Dell'Aversana C, Altucci L, Mai A, Capogrossi MC, Puri PL, Gaetano C. HDAC2 blockade by nitric oxide and histone deacetylase inhibitors reveals a common target in Duchenne muscular dystrophy treatment. Proc Natl Acad Sci U S A. 2008 Dec 9; 105 (49) :19183-7.
• Daubas P, Crist CG, Bajard L, Relaix F, Pecnard E, Rocancourt D, Buckingham M. The regulatory mechanisms that underlie inappropriate transcription of the myogenic determination gene Myf5 in the central nervous system. Dev Biol. 2009 Mar 1; 327 (1) :71-82.
• De Angelis FG, Sthandier O, Berarducci B, Toso S, Galluzzi G, Ricci E, Cossu G, Bozzoni I. Chimeric snRNA molecules carrying antisense sequences against the splice junctions of exon 51 of the dystrophin pre-mRNA induce exon skipping and restoration of a dystrophin synthesis in Delta 48-50 DMD cells. Proc Natl Acad Sci U S A. 2002 Jul 9; 99 (14) :9456-61.
• Denti MA, Rosa A, D'Antona G, Sthandier O, De Angelis FG, Nicoletti C, Allocca M, Pansarasa O, Parente V, Musarò A, Auricchio A, Bottinelli R, Bozzoni I. Body-wide gene therapy of Duchenne muscular dystrophy in the mdx mouse model. Proc Natl Acad Sci U S A. 2006 Mar 7; 103 (10) :3758-63.
• Denti MA, Incitti T, Sthandier O, Nicoletti C, De Angelis FG, Rizzuto E, Auricchio A, Musarò A, Bozzoni I. Long-term benefit of adeno-associated virus/antisense-mediated exon skipping in dystrophic mice. Hum Gene Ther. 2008 Jun; 19 (6) :601-8.
• Donà M, Sandri M, Rossini K, Dell'Aica I, Podhorska-Okolow M, Carraro U. Functional in vivo gene transfer into the myofibers of adult skeletal muscle. Biochem Biophys Res Commun. 2003 Dec 26; 312 (4) :1132-8.
• Eisenberg I, Eran A, Nishino I, Moggio M, Lamperti C, Amato AA, Lidov HG, Kang PB, North KN, Mitrani-Rosenbaum S, Flanigan KM, Neely LA, Whitney D, Beggs AH, Kohane IS, Kunkel LM. Distinctive patterns of microRNA expression in primary muscular

disorders. Proc Natl Acad Sci U S A. 2007 Oct 23; 104 (43) :17016-21.
• Ervasti JM, Sonnemann KJ. Biology of the striated muscle dystrophin-glycoprotein complex. Int Rev Cytol. 2008; 265:191-225.
• Fazi F, Rosa A, Fatica A, Gelmetti V, De Marchis ML, Nervi C, Bozzoni I. A minicircuitry comprised of microRNA-223 and transcription factors NFI-A and C/EBPalpha regulates human granulopoiesis. Cell. 2005 Dec 2; 123 (5) :819-31.
• Gentner B, Schira G, Giustacchini A, Amendola M, Brown BD, Ponzoni M, Naldini L. Stable knockdown of microRNA in vivo by lentiviral vectors. Nat Methods. 2009 Jan; 6 (1) :63-6.
• Ghahramani Seno MM, Graham IR, Athanasopoulos T, Trollet C, Pohlschmidt M, Crompton MR, Dickson G. RNAi-mediated knockdown of dystrophin expression in adult mice does not lead to overt muscular dystrophy pathology. Hum Mol Genet. 2008 Sep 1; 17 (17) :2622-32.
• Gupte SA, Levine RJ, Gupte RS, Young ME, Lionetti V, Labinskyy V, Floyd BC, Ojaimi C, Bellomo M, Wolin MS, Recchia FA. Glucose-6-phosphate dehydrogenase-derived NADPH fuels superoxide production in the failing heart. J Mol Cell Cardiol. 2006 Aug; 41 (2) :340-9.
• Haslett JN, Sanoudou D, Kho AT, Bennett RR, Greenberg SA, Kohane IS, Beggs AH, Kunkel LM. Gene expression comparison of biopsies from Duchenne muscular dystrophy (DMD) and normal skeletal muscle. Proc Natl Acad Sci U S A. 2002 Nov 12; 99 (23) :15000-5.
• Ikeda S, Kong SW, Lu J, Bisping E, Zhang H, Allen PD, Golub TR, Pieske B, Pu WT. Altered microRNA expression in human heart disease. Physiol Genomics. 2007 Nov 14; 31 (3) :367-73.
• Incitti T, De Angelis FG, Cazzella V, Sthandier O, Pinnarò C, Legnini I, Bozzoni I. Exon skipping and duchenne muscular dystrophy therapy: selection of the most active U1 snRNA antisense able to induce dystrophin exon 51 skipping. Mol Ther. 2010 Sep; 18 (9) :1675-82.
• Ivey KN, Muth A, Arnold J, King FW, Yeh RF, Fish JE, Hsiao EC, Schwartz RJ, Conklin BR, Bernstein HS, Srivastava D.

MicroRNA regulation of cell lineages in mouse and human embryonic stem cells. Cell Stem Cell. 2008 Mar 6; 2 (3) :219-29.
• Jung M. Inhibitors of histone deacetylase as new anticancer agents. Curr Med Chem. 2001 Oct; 8 (12) :1505-11.
• Kim HK, Lee YS, Sivaprasad U, Malhotra A, Dutta A. Muscle-specific microRNA miR-206 promotes muscle differentiation. J Cell Biol. 2006 Aug 28; 174 (5) :677-87.
• Koenig M, Beggs AH, Moyer M, Scherpf S, Heindrich K, Bettecken T, Meng G, Müller CR, Lindlöf M, Kaariainen H. The molecular basis for Duchenne versus Becker muscular dystrophy: correlation of severity with type of deletion. Am J Hum Genet. 1989 Oct; 45 (4) :498-506.
• Krol J, Loedige I, Filipowicz W. The widespread regulation of microRNA biogenesis, function and decay. Nat Rev Genet. 2010 Sep; 11 (9) :597-610.
• Krützfeldt J, Rajewsky N, Braich R, Rajeev KG, Tuschl T, Manoharan M, Stoffel M. Silencing of microRNAs in vivo with 'antagomirs'. Nature. 2005 Dec 1; 438 (7068) :685-9.
• Liu N, Williams AH, Kim Y, McAnally J, Bezprozvannaya S, Sutherland LB, Richardson JA, Bassel-Duby R, Olson EN. An intragenic MEF2-dependent enhancer directs muscle-specific expression of microRNAs 1 and 133. Proc Natl Acad Sci U S A. 2007 Dec 26; 104 (52) :20844-9.
• Matsumura K, Tomé FM, Collin H, Leturcq F, Jeanpierre M, Kaplan JC, Fardeau M, Campbell KP. Expression of dystrophin-associated proteins in dystrophin-positive muscle fibers (revertants) in Duchenne muscular dystrophy. Neuromuscul Disord. 1994 Mar; 4 (2) :115-20.
• McCarthy JJ. MicroRNA-206: the skeletal muscle-specific myomiR. Biochim Biophys Acta. 2008 Nov; 1779 (11) :682-91.
• Minetti GC, Colussi C, Adami R, Serra C, Mozzetta C, Parente V, Fortuni S, Straino S, Sampaolesi M, Di Padova M, Illi B, Gallinari P, Steinkühler C, Capogrossi MC, Sartorelli V, Bottinelli R, Gaetano C, Puri PL. Functional and morphological recovery of dystrophic muscles in mice treated with deacetylase inhibitors. Nat Med. 2006 Oct; 12 (10) :1147-50.

- Morlando M, Ballarino M, Gromak N, Pagano F, Bozzoni I, Proudfoot NJ. Primary microRNA transcripts are processed co-transcriptionally. Nat Struct Mol Biol. 2008 Sep; 15 (9) :902-9.
- Nott A, Watson PM, Robinson JD, Crepaldi L, Riccio A. S-Nitrosylation of histone deacetylase 2 induces chromatin remodelling in neurons. Nature. 2008 Sep 18; 455 (7211) :411-5.
- Pandolfi PP, Sonati F, Rivi R, Mason P, Grosveld F, Luzzatto L. Targeted disruption of the housekeeping gene encoding glucose 6-phosphate dehydrogenase (G6PD): G6PD is dispensable for pentose synthesis but essential for defense against oxidative stress. EMBO J. 1995 Nov 1; 14 (21) :5209-15.
- Pena JT, Sohn-Lee C, Rouhanifard SH, Ludwig J, Hafner M, Mihailovic A, Lim C, Holoch D, Berninger P, Zavolan M, Tuschl T. miRNA in situ hybridization in formaldehyde and EDC-fixed tissues. Nat Methods. 2009 Feb; 6 (2) :139-41.
- Potthoff MJ, Olson EN. MEF2: a central regulator of diverse developmental programs. Development. 2007 Dec; 134 (23) :4131-40.
- Rando TA, Disatnik MH, Yu Y, Franco A. Muscle cells from mdx mice have an increased susceptibility to oxidative stress. Neuromuscul Disord. 1998 Feb; 8 (1) :14-21.
- Rando TA, Blau HM. Primary mouse myoblast purification, characterization, and transplantation for cell-mediated gene therapy. J Cell Biol. 1994 Jun; 125 (6) :1275-87.
- Rao PK, Kumar RM, Farkhondeh M, Baskerville S, Lodish HF. Myogenic factors that regulate expression of muscle-specific microRNAs. Proc Natl Acad Sci U S A. 2006 Jun 6; 103 (23) :8721-6.
- Relaix F, Montarras D, Zaffran S, Gayraud-Morel B, Rocancourt D, Tajbakhsh S, Mansouri A, Cumano A, Buckingham M. Pax3 and Pax7 have distinct and overlapping functions in adult muscle progenitor cells. J Cell Biol. 2006 Jan 2; 172 (1) :91-102.
- Schwartz JC, Younger ST, Nguyen NB, Hardy DB, Monia BP, Corey DR, Janowski BA. Antisense transcripts are targets for activating small RNAs. Nat Struct Mol Biol. 2008 Aug; 15 (8) :842-8.
- Shkryl VM, Martins AS, Ullrich ND, Nowycky MC, Niggli E, Shirokova N. Reciprocal amplification of ROS and Ca(2+) signals

in stressed mdx dystrophic skeletal muscle fibers. Pflugers Arch. 2009 Sep; 458 (5) :915-28.
• Taulli R, Bersani F, Foglizzo V, Linari A, Vigna E, Ladanyi M, Tuschl T, Ponzetto C. The muscle-specific microRNA miR-206 blocks human rhabdomyosarcoma growth in xenotransplanted mice by promoting myogenic differentiation. J Clin Invest. 2009 Aug; 119 (8) :2366-78.
• Tseng BS, Zhao P, Pattison JS, Gordon SE, Granchelli JA, Madsen RW, Folk LC, Hoffman EP, Booth FW. Regenerated mdx mouse skeletal muscle shows differential mRNA expression. J Appl Physiol. 2002 Aug; 93 (2) :537-45.
• Vasudevan S, Tong Y, Steitz JA. Switching from repression to activation: microRNAs can up-regulate translation. Science. 2007 Dec 21; 318 (5858) :1931-4.
• Walker DL, Reid JM, Svingen PA, Rios R, Covey JM, Alley MC, Hollingshead MG, Budihardjo II, Eckdahl S, Boerner SA, Kaufmann SH, Ames MM. Murine pharmacokinetics of 6-aminonicotinamide (NSC 21206), a novel biochemical modulating agent. Biochem Pharmacol. 1999 Sep 15; 58 (6) :1057-66.
• Wang H, Garzon R, Sun H, Ladner KJ, Singh R, Dahlman J, Cheng A, Hall BM, Qualman SJ, Chandler DS, Croce CM, Guttridge DC. NF-kappaB-YY1-miR-29 regulatory circuitry in skeletal myogenesis and rhabdomyosarcoma. Cancer Cell. 2008 Nov 4; 14 (5) :369-81.
• Williams AH, Liu N, van Rooij E, Olson EN. MicroRNA control of muscle development and disease. Curr Opin Cell Biol. 2009 Jun; 21 (3) :461-9.
• Williams AH, Valdez G, Moresi V, Qi X, McAnally J, Elliott JL, Bassel-Duby R, Sanes JR, Olson EN. MicroRNA-206 delays ALS progression and promotes regeneration of neuromuscular synapses in mice. Science. 2009 Dec 11; 326 (5959) :1549-54.
• Yuasa K, Hagiwara Y, Ando M, Nakamura A, Takeda S, Hijikata T. MicroRNA-206 is highly expressed in newly formed muscle fibers: implications regarding potential for muscle regeneration and maturation in muscular dystrophy. Cell Struct Funct. 2008; 33 (2) :163-9.

• Zhao Y, Samal E, Srivastava D. Serum response factor regulates a muscle-specific microRNA that targets Hand2 during cardiogenesis. Nature. 2005 Jul 14; 436 (7048) :214-20.
• van Rooij E, Liu N, Olson EN. MicroRNAs flex their muscles. Trends Genet. 2008 Apr; 24 (4) :159-66.
• van Rooij E, Sutherland LB, Liu N, Williams AH, McAnally J, Gerard RD, Richardson JA, Olson EN. A signature pattern of stress-responsive microRNAs that can evoke cardiac hypertrophy and heart failure. Proc Natl Acad Sci U S A. 2006 Nov 28; 103 (48) :18255-60.
• van Rooij E, Sutherland LB, Thatcher JE, DiMaio JM, Naseem RH, Marshall WS, Hill JA, Olson EN. Dysregulation of microRNAs after myocardial infarction reveals a role of miR-29 in cardiac fibrosis. Proc Natl Acad Sci U S A. 2008 Sep 2; 105 (35) :13027-32.

LIST OF PUBLICATIONS - D. Cacchiarelli -

- **Cacchiarelli D**, Incitti T, Martone J, Cesana M, Cazzella V, Santini T, Sthandier O and Bozzoni I. *miR-31 modulates dystrophin expression in human and murine myoblasts: novel implications in Duchenne Muscular Dystrophy*.
  EMBOR. Accepted

- **Cacchiarelli D**, Martone J, Girardi E, Cesana M, Incitti T, Morlando M, Nicoletti C, Santini T, Sthandier O, Barberi L, Auricchio A, Musarò A, Bozzoni I. *MicroRNAs involved in molecular circuitries relevant for the Duchenne muscular dystrophy pathogenesis are controlled by the dystrophin/nNOS pathway.*
  Cell Metab. 2010 Oct 6;12(4):341-51. Epub 2010 Aug 19.

- Ballarino M, Pagano F, Girardi E, Morlando M, **Cacchiarelli D**, Marchioni M, Proudfoot NJ, Bozzoni I. *Coupled RNA processing and transcription of intergenic primary microRNAs.*
  Mol Cell Biol. 2009 Oct;29(20):5632-8. Epub 2009 Aug 10.

- **Cacchiarelli D**, Santoni D, Bozzoni I. *MicroRNAs as prime players in a combinatorial view of evolution.*
  RNA Biol. 2008 Jul-Sep;5(3):120-122. Epub 2008 Jul 8.

- Pavoni E, **Cacchiarelli D**, *Tittarelli R, Orsini M, Galtieri A, Giardina B, Brancaccio A. Duplication of the dystroglycan gene in most branches of teleost fish.*
  BMC Mol Biol. 2007 May 17;8:34.